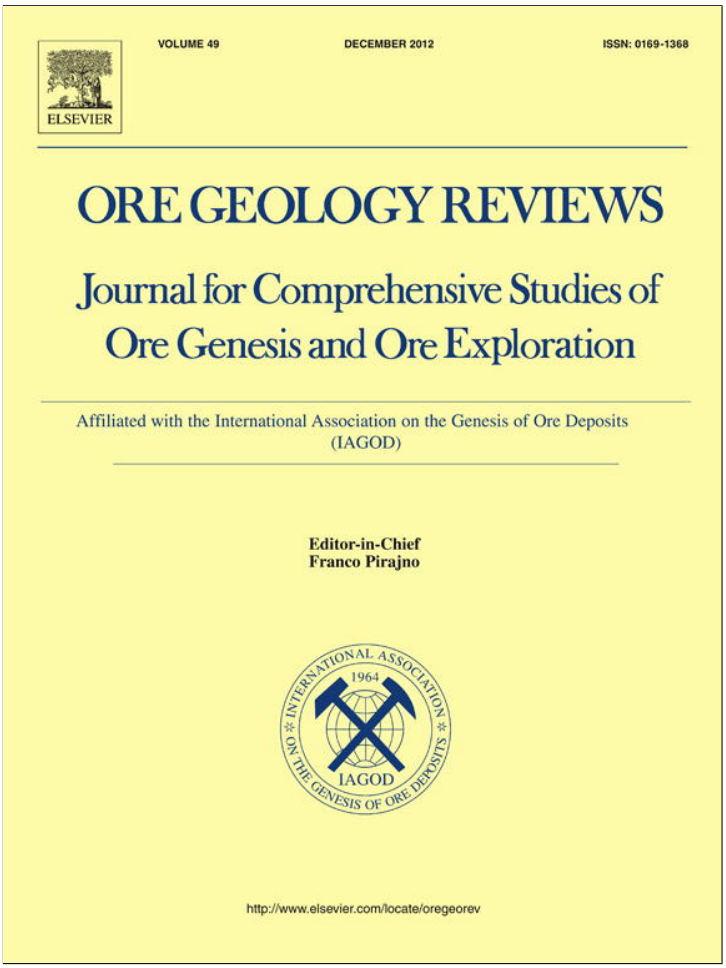

Ore Geology Reviews 49 (2012) 45–71

Contents lists available at SciVerse ScienceDirect

Ore Geology Reviews

journal homepage: www.elsevier.com/locate/oregeorev

Review

The mechanics of hydrothermal systems: II. Fluid mixing and chemical reactions

Daniel R. Lester [a], Alison Ord [b,*], Bruce E. Hobbs [b,c]

[a] CSIRO Mathematics, Informatics and Statistics, Graham Rd, Highett, VIC 3190, Australia
[b] School of Earth and Environment, University of Western Australia, 35 Stirling Highway, Crawley, Perth WA 6009, Australia
[c] CSIRO Earth Science and Resource Engineering, PO Box 1130, Bentley, WA 6102, Australia

ARTICLE INFO

Article history:
Received 28 May 2012
Received in revised form 13 July 2012
Accepted 17 August 2012
Available online 25 August 2012

Keywords:
Hydrothermal systems
Chaotic mixing
Open flow systems
Flow controlled systems
Mineralisation
Ergodicity
Multifractals

ABSTRACT

In the accompanying paper, Part I, hydrothermal mineralising systems are considered as open chemical reactors that operate far from equilibrium to develop an exothermal alteration system with veining and brecciation, followed by competition between endothermic mineralisation and exothermic mineral reactions. In this sequel paper, we examine the interplay of these processes with fluid transport and the impact upon mineral deposition. Chemical reaction and flow in porous media admit two distinct mechanisms which result in significantly accelerated mixing. First, gradients in physical parameters such as chemical potential, fluid density and surface tension generate flow instabilities which form fluid/chemical *mixing machines* that propagate with the reaction front. Second, so-called *chaotic advection*, a behaviour in which fluid particles follow chaotic trajectories, arises inherently from Stokes flow in open porous networks as a result of the complexity of the pore geometry. For pore length-scales greater than ~1 mm, these mechanisms significantly enhance mixing and hence metal/sulphide deposition. Furthermore, chaotic advection can also alter qualitative characteristics such as stability or speciation of non-equilibrium chemical reactions, with significant implications for enhanced mineralisation rates. Such interactions between chemical reaction and fluid advection generate mineral deposits with multifractal spatial signatures similar to those observed in the field. Such multifractal signatures render the spatial distributions *non-ergodic*, a fact which *process based geostatistics* must take into account.

Contents

* Corresponding author.
E-mail address: alison.ord@uwa.edu.au (A. Ord).

0169-1368/$ – see front matter © 2012 Elsevier B.V. All rights reserved.
http://dx.doi.org/10.1016/j.oregeorev.2012.08.002

1. Introduction

Many mineralised hydrothermal systems are characterised by strong spatial gradients in chemical potential, specifically expressed as redox/pH fronts. Examples include *inter alia* the gold systems of Western Australia (Neumayr et al., 2005, 2008) and of the Witwatersrand (Barnicoat et al., 1997) and the iron oxide–copper–gold (IOCG) deposit at Olympic Dam (Haynes et al., 1995). Such fronts occur at all spatial scales (see Part I) ranging over 15 orders of magnitude from the nano-scale (Reich et al., 2005) to the regional scale (Neumayr et al., 2005, 2008; Prendergast, 2007). Mixing of two or more fluids of completely different sources has been proposed to account for such gradients (Appold and Garven, 2000; Haynes et al., 1995; Neumayr et al., 2005, 2008; Prendergast, 2007). In addition, a patterned distribution of mineralogy is observed both inside and outside the ore body. The alteration envelope is commonly very large (tens of cubic kilometres or larger) compared to the mineralised parts of the system. Examples are given by Dube and Goselin (2007), Eastoe et al. (1987), Large et al. (2001), and Muntean et al. (2011). The zoned distribution of mineralisation is commonly associated with brecciation or stockwork structures (Oreskes and Einaudi, 1990). The result is an apparently irregular distribution of mineralisation within the ore body that is reflected as a multifractal distribution (Arias et al., 2011; Bastrakov et al., 2007; Ford and Blenkinsop, 2009; Hunt et al., 2007; Li et al., 2009; Oreskes and Einaudi, 1990; Qingfei et al., 2008; Riedi, 1998; Sanderson et al., 2008). Fractal (or at least, power law) distributions of mineralisation are reported by Carlson (1991) and Schodde and Hronsky (2006). A challenge is to understand such mixing effects and mechanisms over the large range of spatial scales mentioned above, and link these effects with observed spatio-temporal signatures of mineral deposition. Understanding these processes allows greater insight into the deposition process and aids the prediction of large ore deposits associated with hydrothermal systems.

Although fluid mixing is widely proposed as an important ingredient in the formation of hydrothermal systems, it remains very poorly understood (Ord et al., 2010). We describe fluid mixing as the dispersion of constituent species through the actions of fluid advection and/or molecular diffusion toward a spatially homogeneous distribution. Mixing of two fluids can occur in three ways: (i) two laminar flowing fluid streams may meet and mix by diffusion across the interface between the fluids; (ii) differences in the chemical or physical properties of the two fluid streams (for instance chemical potential, density, surface tension, temperature) generate flow instabilities which enhance fluid mixing; (iii) two fluid streams may meet in an open three dimensional network, either at the grain-scale where the network comprises a series of interconnected pores between grains or at larger scales where the network comprises a series of interconnected open fractures. The inherent three dimensional geometric complexity of these networks results in a flow phenomenon known as "chaotic advection", that is, fluid particle trajectories form a chaotic tangle, leading to efficient mixing. The first mixing mechanism involves diffusion alone, and is not efficient as the molecular diffusivity, D, for relevant aqueous species is typically of magnitude 10^{-10} m^2 s^{-1}, as discussed further in Section 4 and also by Appold and Garven (2000). The latter two mechanisms involve the interplay of advection and diffusion, the relative timescales of which are characterised by the Péclet number, Pe,

$$\mathrm{Pe} = \frac{\mathrm{Lv}}{\mathrm{D}} \tag{1.1}$$

where L and v respectively are the characteristic length and fluid velocity scales of the system.

We briefly explore the influence of Pe on mixing behaviour in order to set the framework for the remainder of this paper. In what follows we use the term *pore* to mean any fluid filled space in the rock mass. At the grain scale this commonly arises from the irregular packing of grains but at larger scales it corresponds to open fractures. As an example of the control that Pe exerts on the types of mixing and chemical processes that operate, we assume the permeability, K, is given in terms of the porosity, ϕ, as

$$\mathrm{K} = \alpha\left(\frac{\phi}{\phi_o}\right)^3$$

where α is a constant that we take to be 10^{-18} m^2. We also assume $\phi_o = 10^{-2}$ so that $\mathrm{K} = 10^{-18}$ m^2 when $\phi = 10^{-2}$. This gives a realistic range of porosities for K between 10^{-18} m^2 and 10^{-13} m^2, the range of geologically realistic permeabilities for the mid-crust (see also Manning and Ingebritsen, 1999). Now the real fluid velocity is $\mathrm{v} = \frac{\hat{\mathrm{V}}}{\phi}$ where $\hat{\mathrm{V}}$ is the Darcy velocity, and so

$$|\mathrm{v}| = \frac{\mathrm{K}}{\mu\phi}\nabla\mathcal{H} = \frac{\mathrm{K}^{2/3}\sqrt[3]{\alpha}}{\mu\phi_o}\nabla\mathcal{H}$$

where μ is the fluid viscosity and $\nabla\mathcal{H}$ is the gradient in hydraulic potential.

As an upper limit for the gradient in hydraulic potential we assume the fluid pressure is lithospheric with a rock density of 2700 kg m^{-3} and $\mu = 10^{-3}$ Pa s. Then

$$|\mathrm{v}| = \mathrm{K}^{2/3} \times 1.7 \times 10^3.$$

For chaotic mixing to influence chemical reaction rates (Lester, submitted for publication; Ottino, 1990; Tel et al., 2000), the Péclet number, Pe, is taken to be

$$\mathrm{Pe} = \frac{\mathrm{Lv}}{\mathrm{D}} > 10^2$$

where $\mathrm{D} = 10^{-10}$ m^2 s^{-1} is the diffusivity of chemical species in the fluid. Thus for chaotic mixing to enhance chemical reaction rates significantly,

$$\frac{\mathrm{LK}^{2/3}\sqrt[3]{\alpha}}{\mu\phi_o\mathrm{D}}\nabla\mathcal{H} > 10^2.$$

The variation of L with K is given in Fig. 1.1. Below the line marked $\mathrm{Pe} = 1$ chemical reactions are dominated by reaction–diffusion processes. Chaotic mixing involving laminar flow occurs in the range $1 < \mathrm{Pe} < 10^7$ but enhanced chemical reaction rates due to chaotic flow

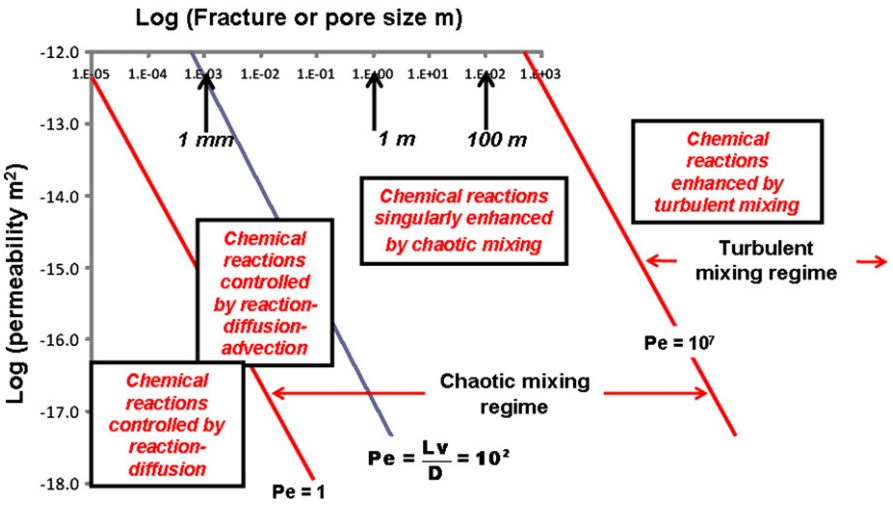

Fig. 1.1. Regimes of laminar and turbulent flow defined in log(permeability) − log(fracture or pore size) space by the Peclet number, Pe. The plot is for a lithostatic fluid pressure gradient. For $Pe<1$ reaction diffusion processes dominate. For $1<Pe<10^7$ chaotic mixing occurs. For $1<Pe<10^2$ chaotic mixing means that reactions are still dominated by reaction–diffusion-advection processes. For $10^2<Pe<10^7$ chaotic mixing means that chemical reactions are singularly enhanced by chaotic mixing. For $Pe>10^7$ turbulent mixing dominates.

occur only for $10^2<Pe<10^7$. Turbulent mixing begins at $Pe=10^7$ (Villermaux, 2012), corresponding to a Reynolds number of 10^3 (see Eq. (3.1)). Turbulent flow still results in enhanced chemical reaction rates (Villermaux, 2012) but one sees from Fig. 1.1 that turbulent flow is unlikely given the assumptions made above. The fact that L becomes smaller for larger permeabilities reflects the faster fluid velocities at higher permeabilities. Similarly, L becomes larger as the hydraulic potential gradient decreases towards hydrostatic, and fluid velocities decrease to zero. The smaller the bulk permeability, the greater the fracture length required before such enhancement occurs.

Below the threshold $Pe=1$, the effect of fluid advection upon mixing is negligible and diffusion dominates, whereas above the threshold $Pe=10^2$ advection can enhance mixing rates by several orders of magnitude. Fluid advection not only has a profound effect upon mixing rates, but can also alter the stability and speciation of non-equilibrium chemical reactions (Tel et al., 2005) such as those encountered in hydrothermal systems. Hence the threshold Péclet numbers not only represent approximate thresholds in terms of mixing rate, but also the qualitative properties of mineral deposition are expected to differ across these thresholds. Although fluid advection is important below $Pe=10^2$ for transporting, reacting mineralizing systems, the argument above suggests that these latter systems may be validly treated as reaction–diffusion (RD) systems which translate through space. Although the literature on RD systems is immense, advection–diffusion–reaction (ADR) systems have enjoyed much less attention, and it is the properties of these systems in the context of hydrothermal systems which is the focus of this study. As such, we are chiefly concerned with the role that fluid advection plays in connection with mixing and chemical reaction, and so the bulk of our discussion is relevant for permeabilities greater than 10^{-18} m^2 and with fracture lengths greater than 1 mm unless mentioned otherwise.

In an accompanying paper, Part I, we considered non-equilibrium chemical systems representative of hydrothermal systems which involve autocatalytic reactions, exothermic thermocatalytic reactions and heterogeneous reaction kinetics. When reactants are well-mixed, the associated chemical reactions may exhibit a range of dynamics including steady, multi-stable, oscillatory and chaotic behaviour. In this paper, Part II, we extend these concepts to the case where reactants are not well mixed, and so have heterogeneous spatial distributions which can significantly influence both physical and chemical phenomena in hydrothermal systems, which in turn impacts mineral deposition. Clearly the interplay of fluid mixing and reactions is relevant here, and it must be stressed that whilst mixing eventually leads to homogeneous well-mixed concentration distributions, simultaneous fluid mixing and reaction involves partially mixed constituents with very different concentration distributions (displaying as highly striated, complex filaments) to that of the well-mixed state. The difference is that these distributions can lead to profound changes in the coupled transport and reaction dynamics, and the associated spatial signatures of mineral deposition.

The paper is organized as follows. In Section 2 we define the relevant governing equations and dimensionless groups for coupled advection, diffusion and reaction in hydrothermal systems. In Section 3 we provide a brief overview of the concepts of chaotic advection with respect to fluid mixing and transport. Section 4 considers the influence of chemical reactions on fluid properties such as density, viscosity and surface tension, and the effects of these changes upon flow instabilities and fluid mixing. In Section 5 we consider how both steady flow in open porous networks, and transient flow at larger scales can generate chaotic advection and fluid mixing in hydrothermal systems. As Sections 4 and 5 provide evidence for the propensity for chaotic advection to occur in hydrothermal systems, Section 6 reviews the impacts of chaotic advection upon non-equilibrium chemical reactions relevant to mineralisation processes. Sections 7 and 8 discuss the implications of coupled fluid mixing and reaction in hydrothermal systems for the spatial distribution of mineral deposition, and the relevance of these findings for both mineral exploration and geostatistics. Terms and symbols are defined as they are first used and in Table A1 in the Appendix. Some equations are repeated in slightly different forms in various sections so that each section is more or less independent of other sections.

2. Governing equations and definition of terms

This section outlines some of the concepts and terms that may be unfamiliar to the geoscientist but are useful in discussing fluid mixing and coupled chemical reactions. Extended treatments of the subject are given by Ottino (1989), Tel et al. (2000, 2005) and Metcalfe (2010). A useful discussion of some of the terms used in chaotic mixing is Wiggins and Ottino (2004) and it is recommended prior reading for Section 3.

2.1. Governing equations

Mineralisation reactions in hydrothermal systems involve the coupled processes of fluid advection, molecular diffusion and chemical

reaction across a range of ϰ aqueous chemical species. We formalize these concepts by posing the advection–diffusion–reaction (ADR) system for the i-th species whose concentrations c_i evolve as

$$\frac{\partial c_i}{\partial t} + \mathbf{v}\cdot\nabla c_i = \frac{1}{Pe_i}\nabla^2 c_i + Da_i F_i \tag{2.1}$$

where F_i quantifies the reaction kinetics of species i as a function of the concentration of the constituent species

$$F_i = F_i(c_1, c_2, \ldots, c_\kappa) \tag{2.2}$$

v is the velocity field (v_x, v_y, v_z), and Pe_i, Da_i are the Péclet and Damköhler numbers (see Table 2.1) of species i, the latter of which characterises the relative timescales of reaction rate k_i and advection

$$Da_i = \frac{k_i L}{v}. \tag{2.3}$$

As described in Part I, the set of reactions F_i describing the mineralisation process may admit multi-stationary states, and it is useful to examine reduced forms of the full ADR system (2.1) to infer the stability characteristics of mineralisation. The simplest form of Eq. (2.1) which still captures the essential physics of transport and reaction is the 1-D reaction diffusion equation in a closed system:

$$\frac{\partial c_i(x,t)}{\partial t} = D_i\frac{\partial^2 c_i(x,t)}{\partial x^2} + f(c_i) \tag{2.4}$$

or

$$\frac{\partial \boldsymbol{c}(\mathbf{r},t)}{\partial t} = \mathbf{D}\nabla^2\boldsymbol{c}(\mathbf{r},t) + \mathbf{f}(\boldsymbol{c},b) \tag{2.5}$$

where $\boldsymbol{c}(\mathbf{r},t)$ is the local concentration vector at the position defined by **r**, $\mathbf{f}(\boldsymbol{c},b)$ is a vector function representing the reaction kinetics, b stands for a set of control parameters that governs the stability of the chemical system and **D** is the matrix of constant diffusive transport coefficients. As indicated in Section 1 we expect the behaviour described by Eqs. (2.4) and (2.5) to dominate for Pe<1 which corresponds for instance to permeabilities less than 10^{-18} m^2 s^{-1} for fracture/pore length scales less than 1 mm.

The first term on the right hand side of Eqs. (2.4) and (2.5), in which D_i (m^2 s^{-1}) is the diffusion coefficient, describes the change in composition resulting from diffusion. The second term indicates that there are chemical reactions also occurring which affect the concentration of each species (Borckmans et al., 2002; Pojman, 1990). Even at this stage, one can assume some homogeneous steady state (HSS) of reference. A linear stability analysis of the HSS then provides the threshold conditions for instability, and also the order of magnitude of the characteristic wave number of any emerging structure. Derivation and analysis of the *amplitude equations* for the active spatial (Fourier) modes allows for the construction of bifurcation diagrams and pattern selection (Borckmans et al., 2002; Cross and Greenside, 2009; Epstein and Pojman, 1998). We explore nonlinear kinetic models for $\mathbf{f}(\boldsymbol{c}, b)$ of the type discussed in Section 6 of Part I.

In an open flow system with chemical reactions coupled to diffusion, the dynamics are described (Scott, 1994) by

$$\frac{\partial \boldsymbol{c}(\mathbf{r},t)}{\partial t} = \mathbf{D}\nabla^2\boldsymbol{c}(\mathbf{r},t) + \mathbf{f}(\boldsymbol{c},b) + \frac{(\boldsymbol{c}_0-\boldsymbol{c})}{\tau} \tag{2.6}$$

where $\boldsymbol{c}_0$ and $\boldsymbol{c}$ are the concentrations of the species respectively in the input flow and within the reactor and τ is the residence time of the system. If $\mathbf{f}(\boldsymbol{c}, b)$ is nonlinear, combinations of $\mathbf{f}(\boldsymbol{c}, b)$ with either of the other two terms on the right hand side of Eq. (2.6) may give rise to bistability of the HSS or more complicated nonlinear forms of behaviour discussed in Part I and Section 5 in this paper. $(\boldsymbol{c}_0-\boldsymbol{c})/\tau$ is called a *feeding* term. Eq. (2.6) is the same form as Eq. (2.9) in Part I. We expect Eq. (2.6) to be relevant for Pe>1 in Fig. 1.1.

To include transport (De Wit, 2008) the evolution of the Darcy fluid flow velocity $\hat{\mathbf{V}}$ inside the control volume can be described

Table 2.1
Dimensionless groups.

Name	Symbol	Description	Definition
Damköhler number	Da	$\frac{\text{hydrodynamic time scale}}{\text{chemical time scale}}$	$Da = \frac{k_i L}{v}$
Lewis number	Le	$\frac{\text{thermal diffusion coefficient}}{\text{molecular diffusion coefficient}}$	$Le = \frac{\kappa}{D}$
Marangoni number	Mg	$\frac{(\text{thermal}-)\text{surface tension forces}}{\text{viscous forces}}$	$Mg = -\frac{d\sigma}{dT}\cdot\frac{1}{\mu\alpha}\cdot L\cdot\Delta T$
Péclet number	Pe	$\frac{\text{rate of advection}}{\text{rate of diffusion}}$	$Pe^{heat} = Lv/\alpha$ $Pe^{mass} = Lv/D$
Rayleigh number	Ra	$\frac{\text{buoyancy}}{\text{viscosity}}\cdot\frac{\text{momentum diffusivity}}{\text{thermal diffusivity}}$	$Ra = \beta\Delta T L^3 g\frac{K\mu}{\rho^2 c_p}$
Solutal Rayleigh numbers	R_C	$\frac{\text{solutal buoyancy}}{\text{viscosity}}\cdot\frac{\text{momentum diffusivity}}{\text{thermal diffusivity}}$	$R_C = -\frac{\partial\rho}{\partial c}\frac{a_o L_c^3 g}{D\mu}$ Rongy and De Wit (2009) $R_C = \frac{gK\Delta\rho_C}{\mu U}$ D'Hernoncourt et al. (2007)
Thermal Rayleigh numbers	R_T	$\frac{\text{thermal buoyancy}}{\text{viscosity}}\cdot\frac{\text{momentum diffusivity}}{\text{thermal diffusivity}}$	$R_T = -\frac{\partial\rho}{\partial T}\frac{\Delta T L_C^3 g}{D\mu}$ Rongy and De Wit (2009) $R_T = \frac{gK\Delta\rho_T}{\mu U}$ D'Hernoncourt et al. (2007)
Reynolds number	Re	$\frac{\text{fluid inertial forces}}{\text{viscous forces}}$	$Re = \frac{\rho^{fluid} vL}{\mu}, Re = \frac{Pe}{Sc}$
Schmidt number	Sc	$\frac{\text{viscous diffusion}}{\text{molecular diffusion}}$	$Sc = \frac{\mu}{\rho^{fluid} D}$

along with the incompressibility condition or continuity equation $\nabla\cdot\hat{\mathbf{V}} = 0$ (Nagatsu and De Wit, 2011) by Darcy's law

$$\hat{\mathbf{V}} = \left(\rho\mathbf{g} - \nabla P^{\text{fluid}}\right)\frac{K}{\mu} \tag{2.7}$$

where ∇P^{fluid} is the gradient of fluid pressure, $\rho\mathbf{g}$ is a buoyancy force term, where $\mathbf{g}$ is the acceleration due to gravity, μ, ρ are the viscosity (Pa s) and density (kg m^{-3}) of the fluid and K (m^2) is the permeability.

3. Fluid mixing and chaotic advection

3.1. Chaotic advection in laminar flow

In order to understand the mechanisms by which fluid advection accelerates fluid mixing in hydrothermal systems, in this Section we provide a brief overview of the phenomenon of *chaotic advection*, involving terms and concepts which may be unfamiliar to the geoscientist. As indicated above, the reader is directed to several review articles (Metcalfe, 2010; Ottino, 1989; Tel et al., 2000, 2005; Wiggins and Ottino, 2004) for further reading.

The ability of turbulent flow rapidly to mix and disperse constituents is a widely recognized phenomenon (Villermaux, 2012). Turbulent flows possess a wide spectrum of eddy length-scales, which act to distort concentration fields into complex spatial distributions with very fine striations and large interfacial area between constituents of the flow. In conjunction with molecular diffusion, such fluid advection leads to rapid dispersion, which is commonly termed mixing. Dispersion occurs even if the molecular diffusivity is vanishingly small. Conversely, slow, laminar flows typically found in porous and fractured networks are smooth and regular, and do not possess small length scales for the organization of fluid elements into fine striations. As such, slow molecular diffusion usually does little to accelerate dispersion in laminar flows. The transition from laminar to turbulent flow typically occurs at Reynolds number $Re \sim 10^3$, a dimensionless group (Table 2.1) which quantifies the ratio of inertial to viscous forces

$$Re = \frac{Pe}{Sc} \tag{3.1}$$

where $Sc = \mu/\rho^{\text{fluid}}D$ is the Schmidt number quantifying the ratio of viscous diffusion to molecular diffusion; ρ^{fluid} and μ are the fluid density and viscosity respectively. The Schmidt number is a material property, typically 10^4 for aqueous systems (as $\rho^{\text{fluid}} \sim 10^3$ kg m^{-3}, $\mu \sim 10^{-3}$ Pa s, $D \sim 10^{-10}$ m^2 s^{-1}), and so $Re = 10^{-4}$ Pe. Based on the arguments presented in Section 1 (Fig. 1.1) laminar flow is expected for pore/fracture sizes, L_{max}, up to 10^8 times the threshold, L_{min}, above which advection significantly enhances fluid mixing. This means (Fig. 1.1) that turbulent flow is not expected (for a lithospheric hydraulic potential gradient) in the crust for realistic permeabilities.

Based upon such reasoning, one might reasonably conclude that porous media flows for $L < L_{max}$ are smooth and regular and lead to concentration distributions associated with slow dispersion. Whilst this may be true for a wide range of laminar flows, there exist important exceptions. These exceptions arise due to the fact that the kinematic advection equation

$$\frac{d\boldsymbol{x}}{dt} = \mathbf{v}(\boldsymbol{x}, t) \tag{3.2}$$

describing the evolution with time t of the position $\boldsymbol{x}$ of a passive fluid tracer particle under the action of the fluid velocity field $\mathbf{v}$, is a nonlinear dynamical system capable of exhibiting chaotic dynamics. As such, although the velocity field $\mathbf{v}(\boldsymbol{x}, t)$ itself is smooth, the fluid particle trajectories may be chaotic, leading to rapid dispersion and mixing. This phenomenon is termed *chaotic advection* (Aref, 1984; Ottino, 1990), and has been well studied over the past quarter century in the fields of fluid mechanics and dynamical systems.

One familiar example of chaotic advection is the kneading of bread dough or the manufacture of salt-water taffy. Kneading may be considered as a laminar flow comprising of iterated stretching and folding motions. Although the flow field associated with these motions is smooth and regular, if one were to track the evolution of a dyed element of dough or taffy, it would soon be stretched to form a highly striated distribution and eventually be mixed throughout the dough or taffy form. This is chaotic advection in action.

The actions of stretching and folding are in fact the fundamental mechanisms of chaotic dynamics in general: *stretching acts to separate particles at an exponential rate, and folding acts to reorganize the flow to distribute these highly striated interwoven structures throughout the domain*. The rate of exponential stretching is quantified by the Lyapunov exponent λ, which is taken as a measure of the strength of the chaotic dynamics. In the case of chaotic advection, the Lyapunov exponent is defined as the long time limit of the exponential growth rate of the length of a material line $\delta\mathbf{x}$ between two particles initially separated by distance $\delta\mathbf{X}$

$$\lambda \equiv \lim_{t\to\infty}\frac{1}{t}\ln\frac{|\delta\mathbf{x}|}{|\delta\mathbf{X}|}. \tag{3.3}$$

Whilst the flow domain may be finite-sized, $|\delta\mathbf{x}|$ can grow without bound due to the interwoven nature of the striations and hence of the initial material line. Although chaotic particle paths appear to be irregular and random, their underlying structures are highly organized and are often self-similar and multifractal (Muzzio et al., 1992). This organizing structure is termed the chaotic template, and active processes within the fluid such as diffusion and reaction play out on this template.

Although many laminar flows are engineered to exhibit chaotic advection to promote mixing and dispersion in a wide variety of applications, chaotic advection can occur in natural flows also. Systems subject to transient forcing or flow reorientation can exhibit chaotic advection, such as the evolution of plankton communities in oceanic currents (Hernandez-Garcia and Lopez, 2004; Karolyi et al., 1999) or the spreading of the gulf oil spill (Mezić et al., 2010; Thiffeault, 2010). Flows in porous media subject to transient forcing have been shown (Jones and Aref, 1988; Lester et al., 2009, 2010; Metcalfe et al., 2010a, 2010b; Trefry et al., 2012; Zhang et al., 2009) to exhibit chaotic advection again due to the stretching and folding motions of the transient flow field. Recent studies (Carrière, 2007; Lester, submitted for publication) have also established the propensity for chaotic advection to occur in porous media under steady flow, via the natural tortuosity of the pore-space. We shall return to these concepts in greater detail in Sections 4 and 5.

In general, chaotic dynamics may not permeate throughout the entire flow domain, but rather "islands" of regular, non-chaotic motion (where $\lambda = 0$) are interspersed with a background "sea" of chaotic motion (where $\lambda > 0$). In the absence of diffusion, material cannot pass between the regular islands and chaotic sea, and so the islands essentially divide the fluid domain into separate sub-domains which only exchange material in the presence of diffusion. Within these islands a blob of dyed fluid is transported and may be moderately deformed but it does not undergo the exponential stretching associated with the chaotic sea. Conversely, particle trajectories in the chaotic domain separate exponentially and wander throughout the entire domain without ever repeating the same orbit. With time chaotic particle orbits visit the entire chaotic region, and so are termed space-filling orbits.

The term *ergodicity* (from the Greek: *wandering*) when applied to dynamic systems, refers to a property of the system whereby the behaviour of the system averaged over time corresponds to the behaviour averaged over space (Adler, 1981). Due to the space-filling

nature of chaotic orbits, a chaotic region within the flow domain has the property of being *ergodic*, a requirement for the definition of a chaotic system (Wiggins and Ottino, 2004). This is reflected in the definition of the Lyapunov exponent λ (Eq. (3.3)), which is a time-averaged measure; as the chaotic region is ergodic, the Lyapunov exponent is constant throughout. However, the same cannot be said for the entire flow domain when non-chaotic islands ($\lambda = 0$) are present. Likewise flows which admit regular islands are deemed to be non-ergodic due to these barriers to transport.

The concept of ergodicity is important from another point of view because it is used by geo-statisticians to perform many forms of spatial prediction or *kriging* (Cressie, 1993). Given a limited set of spatial measurements on ore grade one has to make assumptions about these measurements, such as the way they are related to the mean of the population as a whole or their covariance or other statistical properties, in order to estimate spatial averages of blocks comprising the ore body. The assumption of ergodicity is one commonly used assumption that allows one to proceed. It justifies using spatial averages based on limited data to estimate the covariance function (or semivariogram) and, hence, allows construction of kriging predictors based on limited samples (Cressie, 1993; Cressie and Wikle, 2011). The assumption of ergodicity in geostatistics ensures that the sample mean and covariance converge on these same quantities for the population as a whole. Hence it is of critical importance to determine whether fluid mixing and chemical reactions in hydrothermal systems lead to mineral deposits which are ergodically distributed as this provides the underlying physical basis for ergodic kriging. We consider this concept in greater detail in Section 5 where we point out that chemical reaction coupled with the progressive localisation of flow as hydrothermal systems evolve leads to non-ergodicity and multifractal spatial distributions.

3.2. Chaotic advection and dispersion

The discussion of chaotic advection in the previous subsection is in the absence of additional transport mechanisms such as molecular diffusion. Fluid mixing (dispersion) arises from the interplay of advection and diffusion, and in certain instances chaotic advection can act to impart an exponential increase in the rate of fluid mixing. As chaotic advection creates concentration distributions with vanishingly small striation widths, negligibly small diffusion acts to smear out striations below the length scale $\sqrt{D/\lambda} \sim 10^{-5}$ m.

The interplay of chaotic advection and diffusion results in concentration fields which manifest as spatio-temporal patterns called *strange eigenmodes* (Liu and Haller, 2004; Pierrehumbert, 1994) which decay exponentially toward the well-mixed, homogeneous state. Strange eigenmodes arise from a balance between diffusion and exponential stretching in a chaotic flow. The resulting patterns arise spontaneously and are labelled strange because they persist, fixed in space, and are not swept downstream with the imposed flow. They decay slowly and so they represent fixed spatial sites where mineral reactions are localised. The evolution of a concentration field c in such an environment is governed by the advection–diffusion equation (ADE)

$$\frac{\partial c}{\partial t} + \mathbf{v}\cdot\nabla c = \frac{1}{Pe}\nabla^2 c. \tag{3.4}$$

Solutions to the ADE comprise superposed strange eigenmodes $\varphi_k(\boldsymbol{x},t)$ which decay at characteristic rates ω_k, with $\omega_k \leq \omega_{k+1}$

$$c(\boldsymbol{x},t) = c_0 + \sum_{k=0}^{\infty} \alpha_k \varphi(\boldsymbol{x},t)\exp(-\omega_k t) \tag{3.5}$$

where α_k is the weighting of each eigenmode and c_0 is the average concentration corresponding to the homogeneous state. As such, in a short time the concentration profiles converge toward the dominant eigenmode φ_0, and the asymptotic rate of mixing is characterised by the dominant decay rate ω_0. For $Pe > 10^2$ (corresponding to $L > L_{min}$), this exponential decay rate for chaotic advection may be several orders of magnitude greater than the corresponding rate for regular laminar flows (Adrover et al., 2002a; Lester et al., 2008), and this acceleration scales as $\sqrt{Pe}$. Hence, the impact of chaotic advection upon mixing is profound.

As the finite-time Lyapunov exponent λ is zero within non-chaotic islands, acceleration of mixing in these regions is negligible (as reflected by Eq. (3.6) below). However, diffusion does provide a means to transport mass across these barriers, albeit slowly. In general, whilst the rate of mixing is exponentially accelerated throughout the chaotic region of the flow, non-chaotic islands hamper this acceleration of *global* mixing (that is, mixing throughout the entire flow domain). Such retardation increases with the size of the non-mixing islands, and the rate of global mixing returns toward that of non-chaotic advection. In general, flows which admit chaotic advection and regular islands of length-scale less than $\sqrt{\lambda/D}$ typically exhibit significantly accelerated dispersion.

Exponential acceleration of dispersion is also clearly illustrated by posing the ADE (Eq. (3.4)) in Lagrangian coordinates $\boldsymbol{\zeta}$ following the chaotic trajectories. In Lagrangian coordinates, chaotic advection drives exponential amplification (or retardation) of the molecular diffusivity along unstable (stable) manifolds (Tang and Boozer, 1996, 1999),

$$\frac{\partial c}{\partial t} = \nabla_\zeta\cdot\left(\mathbf{D}_\zeta\cdot\nabla_\zeta c\right), \mathbf{D}_\zeta = D\left(\hat{\mathbf{e}}\hat{\mathbf{e}}\, e^{2\Lambda t} + \hat{\mathbf{s}}\hat{\mathbf{s}}\, e^{-2\Lambda t}\right), \tag{3.6}$$

where Λ is the local finite-time Lyapunov exponent (a local variant of λ) measuring the stretching history and $\hat{\mathbf{e}}, \hat{\mathbf{s}}$ are the unit vectors along the unstable and stable manifold directions respectively. As chaotic advection is typified by a non-zero Lyapunov exponent, all chaotic flows give rise to anomalous transport, exponentially amplified by Λ, as per Eq. (3.6). Although *local* diffusion is both exponentially amplified and retarded respectively in the unstable and stable manifold directions, the net effect of multiple interacting striations results in an exponential amplification of *global* mixing and dispersion. Note there is no convective term in Eq. (3.4) as the diffusion equation is posed in the Lagrangian frame.

In hydrothermal systems chaotic advection can arise through two distinct mechanisms: first via fluid instabilities due to strong gradients in physico-chemical properties, and second from the complex geometry inherent to open porous networks. In both cases, chaotic advection leads to accelerated mixing which can significantly enhance the reaction rate of mineralisation reactions (Arratia and Gollub, 2006). Furthermore the nature of chaotic advection can alter the stability and speciation of non-equilibrium reactions relevant to hydrothermal systems. In Sections 4 and 5 we shall examine how fluid instabilities and the geometry of open porous networks respectively generate chaotic advection, and in Section 6 we shall explore the implications of chaotic advection for mineralisation reactions in hydrothermal systems.

4. Chemical reactions, flow instabilities and fluid mixing

Hydrothermal systems involve the coupled advection, diffusion and reaction of multiple chemical species which are predominantly borne in the fluid phase. In the case where one fluid displaces another in the system, significant variations in the concentration of chemical species and/or temperature can arise at the fluid interface, which translate into strong gradients of the fluid physical properties such as the viscosity, μ, the density, ρ, or the surface tension, γ. Such gradients in fluid properties can generate a range of flow instabilities from the pore-scale to the macro-scale. Most of these instabilities promote fluid mixing over part of the entire fluid domain and in turn, such mixing can enhance chemical reactions.

If a flow instability is driven (or retarded) by the evolution of a particular reaction (for example, changes in heat, chemical potential, surface tension), then the influence of mixing forms a feedback loop which acts further to destabilise (or stabilise) the system. In this Section we review the interplay between chemical reactions and flow instabilities in hydrothermal systems, and establish the effect of such mixing upon the behaviour of the system.

Combinations of density, viscosity and temperature changes can lead to phenomena such as viscous fingering (Saffman–Taylor instability, Saffman and Taylor, 1958), density fingering (Rayleigh–Taylor instability, Rayleigh, 1882; Taylor, 1950) and convection (Rayleigh–Bénard instability, Benard, 1900a, 1900b; Rayleigh, 1916); variations in the surface tension can lead to Marangoni instabilities (De Wit, 2008; Rongy and De Wit, 2006, 2007, 2008). We do not discuss Marangoni instabilities further here but they are presumably important in multi-phase flow. To probe the dynamics of the coupled advection–diffusion–reaction system the evolution equation for the fluid velocity field is coupled to an ADR equation similar to Eq. (2.1). The goal then is to analyse the resultant nonlinear dynamics for various values of the relevant parameters to provide understanding of the time evolution of the system.

One of the simplest forms of this coupling is given by Nagatsu and De Wit (2011) who numerically integrate an ADR system coupling Darcy flow with a concentration dependant viscosity to equations for the evolution of the concentrations of the three chemical components A, B and C. They then complement numerical studies of nonlinear miscible viscous fingering influenced or fully triggered by a simple first order chemical reaction, $A+B\rightarrow C$, by exploring systematically all possible cases, that is, all situations whether the solution of A is less or more viscous than that of B. It is convenient to analyse the behaviour of such systems in terms of a set of dimensionless numbers (Table 2.1), the Damköhler number, Da, the Péclet number, Pe, the Lewis number, Le, and the Rayleigh number, Ra (Nagatsu et al., 2009). Nagatsu and De Wit (2011) assume the reaction to be isothermal and infinitely fast, that is, $Da=\infty$, and that the diffusion coefficients of all species are identical. The influence of chemical reactions is expressed in terms of two *log-mobility ratios* defined by

$$M_b = \ln\left(\frac{\mu_B}{\mu_A}\right), M_c = \ln\left(\frac{\mu_C}{\mu_A}\right). \quad (4.1)$$

Two types of fingering are obtained depending on whether the corresponding nonreactive system of A displacing B is viscously stable or not (Fig. 4.1). If the log-mobility ratio $M_b>0$, the reaction modifies the fingering dynamics already present in the absence of chemical reactions. If $M_b<0$, fingering is fully triggered by the reaction provided the fluid with C is more, $M_c>0$, or less viscous, $M_c<2M_b<0$, than both A and B. The effect of lower values of Da has been explored by Nagatsu et al. (2007, 2009). In general for high Da if the fluid C is more viscous than fluid B the fingering density is larger for the reactive case than for the less-reactive case. The opposite effects can emerge at lower Da.

Rongy and De Wit (2009) address the additional influence of thermal effects on density in buoyancy-driven convection around exothermic fronts travelling in a horizontal system. Such behaviour may be a mechanism for fluid mixing in a Witwatersrand-type mineralising system. Behaviours which may lead to new dynamics include the more rapid diffusion of heat compared to mass, and possible competition between solutal and thermal buoyancy effects even for a thin horizontal flow. Fig. 4.2 shows a horizontally travelling reaction front between two reacting fluids. It is convenient to define two parameters, the thermal Rayleigh number, R_T, and the solutal Rayleigh number, R_C, as indicated in Table 2.1. The changes in density and viscosity may either reinforce each other or compete with each other (Fig. 4.3).

The influence of double diffusive effects on miscible viscous fingering is explored by Mishra et al. (2010) in a 2D horizontal flow.

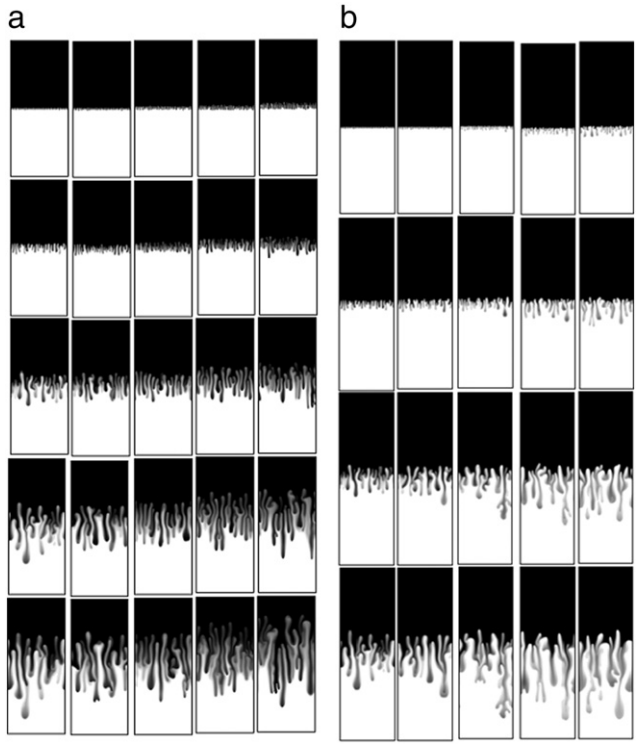

Fig. 4.1. Viscous fingering dynamics involving a simple first order chemical reaction $A+B\rightarrow C$. (a) Fingering for various $M_c\geq M_b=2$ (column 1) to 6 (column 5) shown at dimensionless time $t=400$, 800, 1600, 2400, and 3200 from top to bottom. (b) Same as (a) but $M_c\leq M_b=2$ (column 1) to 6 (column 5). A is black whilst B is white. C forms at the interface between the two.
From Nagatsu and De Wit (2011).

They show that differential diffusion of two components, each contributing to the viscosity of a solvent, can profoundly affect the stability and nonlinear dynamics of viscous fingering. The slow and fast components could for example be mass and heat, or they could be two non-reacting chemical species both influencing the viscosity of

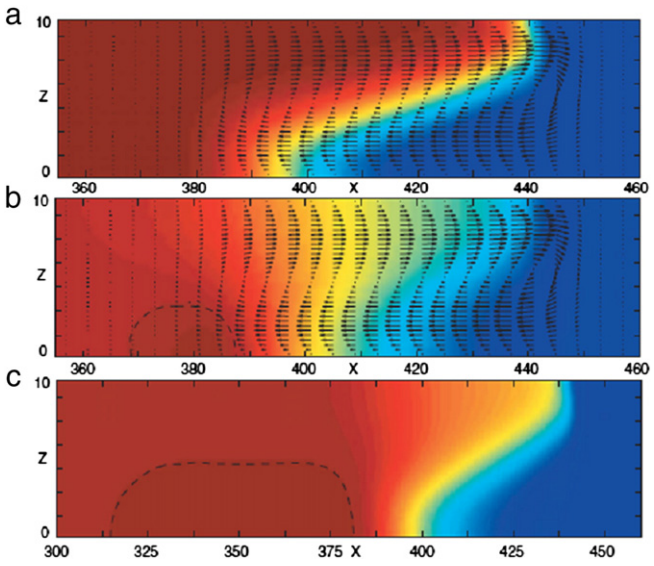

Fig. 4.2. Horizontally travelling convective reaction front for a hotter, less dense fluid invading a colder denser fluid on the right for the cooperative case $R_C=R_T=10$ and $Le=5$ (a) Temperature. (b) Concentration. (c) Zoom into temperature field showing hotter region at base behind the front. The black arrows in (a) and (b) represent the fluid velocity field. For details see Rongy and De Wit (2009).
From Rongy and De Wit (2009).

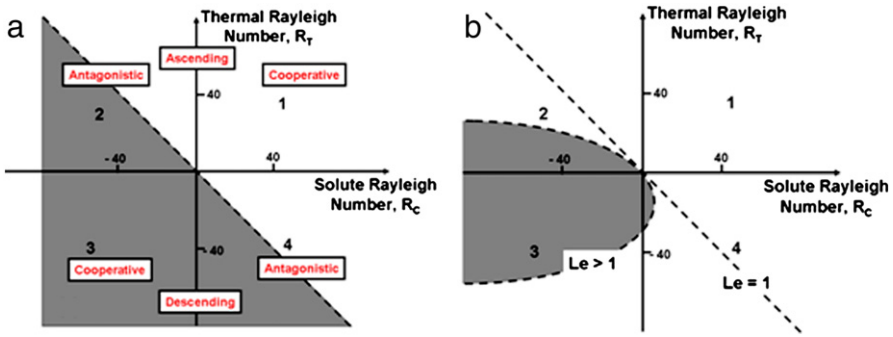

Fig. 4.3. Stability diagram from D'Hernoncourt et al. (2007). R_C and R_T are the solutal and thermal Rayleigh numbers defined in Table 2.1. (a) Plot for Le = 1 (that is, the thermal and molecular diffusion coefficients are equal). The gray area marks out the region of stability. (b) If the Lewis number is greater than 1 the stability area shrinks to the gray area as shown. This opens the possibility for unstable behaviour in unexpected quadrants such as 3 and 4.

the solution but having sufficiently different diffusion coefficients, D_s and D_f respectively. Mishra et al. (2010) define the additional quantities $\delta = D_f/D_s > 1$ and the log mobility ratios $M_f = \ln(D_f/D)$, and $M_s = \ln(D_s/D)$ where D is a reference diffusivity. The behaviour of the system can then be defined in M_f–M_s–δ space. The displacement of a more viscous fluid by a less viscous fluid is classically considered to be stable in the sense that no viscous fingering develops at the interface. Mishra et al. (2010) show that the presence of both fast and slow diffusive species can induce fingering instabilities in these classically stable situations as shown in Fig. 4.4(g, h).

New dynamics arise in vertical geometries where buoyancy-driven instabilities of initially statically stable fronts can occur. Demuth and Meiburg (2003) investigate the linear stability of an upward propagating, unstable density front that separates two chemically reacting fluids in a vertically flow system. Physical experiments were performed by Bockmann and Muller (2000) based on the iodate–arsenous acid reaction. An earlier theoretical investigation by De Wit (2001) was based on Darcy's law whilst the Demuth and Meiburg (2003) investigation is based on the three dimensional Stokes equations. Further developments for such systems are described by De Wit et al. (2003) who study the dynamics of hydrodynamical density fingering of chemical fronts separating two miscible, steady states of different chemical composition and hence of density. The chemical reaction involved at the interface is bistable involving two stationary states labelled c_1 and c_2. Miscible density fingering of chemical fronts in porous media is also described by De Wit (2004) as a reaction–diffusion system. Once chemistry is operative, there is a saturation of its effect as the Damköhler number is further increased. There is a large difference between systems with and without chemical reactions but once reactions are in progress, there is a saturation effect when Da increases past a relatively small value. Thus in Fig. 4.5 the pattern of fingering is much the same for Da = 0.14 as it is for Da = 0.2 whereas there are large differences between Da = 0 (no reaction), Da = 0.01 and Da = 0.04. Increasing the Damköhler number leads to

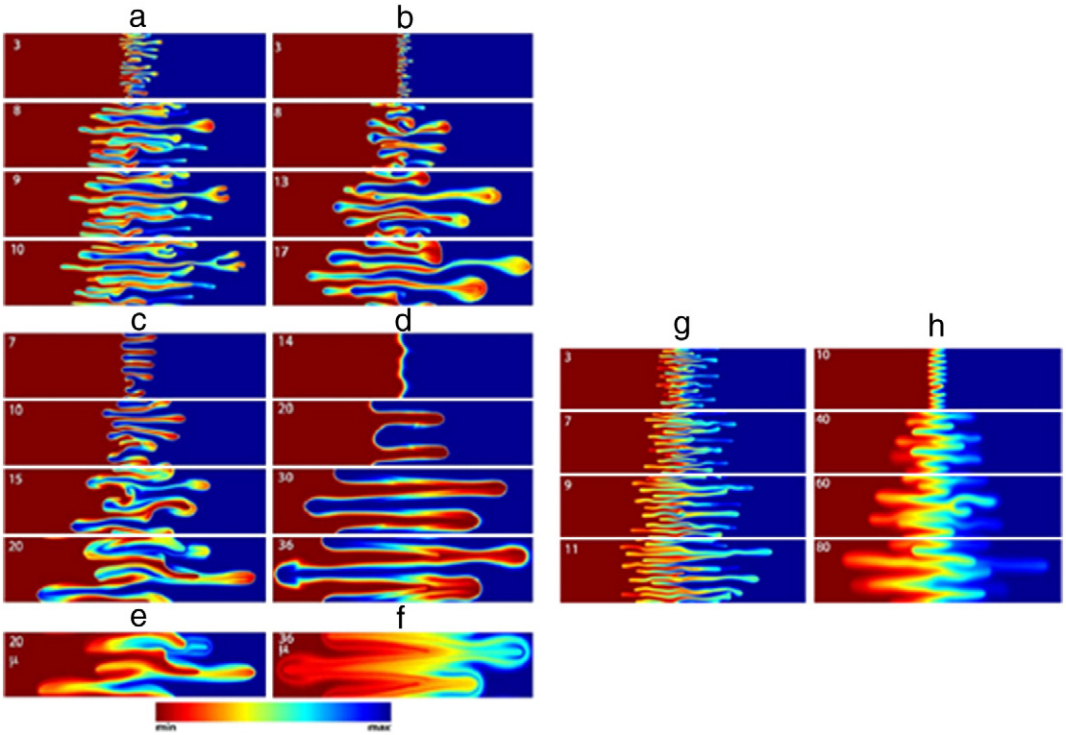

Fig. 4.4. Fingering instabilities of the slow species for (a) $M_s = M_f = \delta = 1$. (b) $M_s = M_f = 1$, $\delta = 10$. (c) $M_s = -1$, $M_f = 3$, $\delta = 4$. (d) $M_s = -1$, $M_f = 3$, $\delta = 10$. (e) and (f) are the viscosity fields corresponding to (c) and (d) respectively. Frames (a) to (f) correspond to "classical" situations where a more viscous fluid invades a less dense fluid. (g) and (h) correspond to situations where a less dense fluid invades a denser fluid and instabilities would not be expected without chemical/hydrodynamic coupling. (g) $M_s = 1$, $M_f = -3.2$, $\delta = 10$. (h) $M_s = -1$, $M_f = 3$, $\delta = 10$. For details see Mishra et al. (2010).
After Mishra et al. (2010).

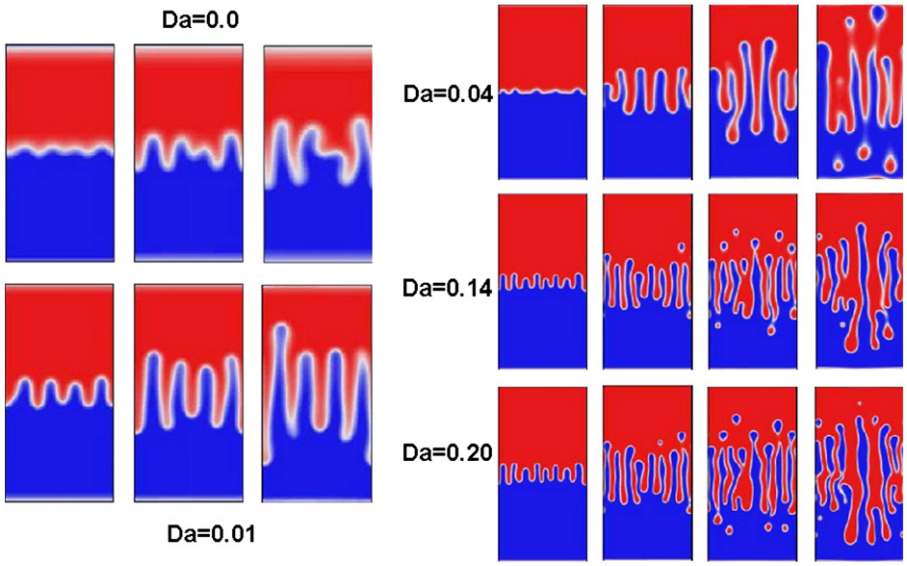

Fig. 4.5. Influence of the Damköhler number on the development of viscous fingering instabilities in chemical reactions with bistability. Pe = 512, d = 0.5, and A = 2. The dimensionless times on the left are t = 1000, 1500, and 2000. The dimensionless times on the right are 500, 1000, 1500 and 2000. Da = 0.0 corresponds to pure viscous fingering. The initiation of a slow reaction increases the lengths of the fingers and decreases the spacing. This trend continues to Da = 0.04 but by Da = 0.14 the patterns tend to stabilise and there is little influence of further increases in Da. The breakup into globules of red in blue and of blue in red at larger time for higher Da represents the influence of bistability. If the reaction involves bistability in pH then each globule and each reaction front represents a pH front. The same is true for reactions involving bistability in Eh.
From De Wit et al. (2003).

sharper fronts travelling with a higher speed (De Wit, 2004). Increasing the Rayleigh number simply leads to larger systems and hence to more fingers (De Wit, 2004). Mixing enhancement greater than factors of 1000 is reported for this system. An important additional feature of the work by De Wit et al. (2003) is the development of isolated globules of the stationary state composition c_1 embedded in c_2 or of c_2 embedded in c_1 at large times and higher values of Da. In the case where these stationary states represent contrast in pH or Eh these globules and the fingering interfaces represent pH or Eh fronts. The detailed mechanisms for the formation of these globules is given by De Wit and Homsy (1999a, 1999b). Rongy and De Wit (2009) also report temporally oscillating fronts in horizontally moving systems.

Under these conditions, stable planar fronts travel with a given constant speed and width. Density fingering (Rayleigh–Taylor instabilities) occurs when the reactant and product solutions have different densities and if the heavier solution lies on top of the lighter one. The Rayleigh–Taylor instability results directly from the dynamics of a buoyantly unstable exothermic front where the front travels vertically (D'Hernoncourt et al., 2007; Pojman and Epstein, 1990). An instability (double-diffusive instability) within the same system may result from the competition between solutal and thermal buoyancy effects (D'Hernoncourt et al., 2007) and the detailed dynamics of these situations is summarised in Fig. 4.3.

Chemical reactions as simple as A + B → C are shown by Almarcha et al. (2010) to trigger instabilities in otherwise stable situations, and also break the symmetry of convective structures and instabilities, based on a general reaction–diffusion-convection model. Fig. 4.6 shows situations where C diffuses at the same rate as the reactants but is denser (Fig. 4.6(a)) and results in a Rayleigh–Taylor instability below the initial contact line which induces convection which pushes the reaction front upwards. In Fig. 4.6(b) two different local instabilities develop with the slower diffusing product C falling downwards through B in Rayleigh–Taylor instabilities and rising plumes of the faster diffusing reactant A above.

Thus the coupling of chemical reactions with the physical properties of the fluids (density, viscosity, surface tension) results in a large array of nonlinear phenomena at the interface between one fluid that is displacing another. Such phenomena can manifest as flow instabilities which result in enhanced mixing in the vicinity of the interface; enhancements of up to 1000-fold have been observed. Such behaviour is expected to occur where one fluid is injected into another or where one fluid displaces another in a fracture. Due to the resultant instabilities, local mixing occurs in the travelling front, forming a chemical "mixing machine" which promotes reaction at the moving interface.

Fluid mixing brought about through these flow instabilities is also a manifestation of chaotic advection. Here the initially smooth fluid interface evolves toward a complex distribution with small-scale structures and exponential growth of the interface in the region of the instability. In most cases the flow instability has a finite lifetime (after which the gradients driving the instability are resolved and the system approaches equilibrium), and so the associated chaotic advection is also of finite lifetime before the flow decays back to the unperturbed state. The motivation for posing the mixing process as a manifestation of chaotic advection is that the effect of chaotic advection extends beyond simply enhancing mixing in these coupled ADR systems. It is now well-established (Tel et al., 2005) that chaotic advection can also alter the stability and speciation of non-equilibrium chemical reactions typical of hydrothermal systems such as autocatalytic and bistable reactions. Although chaotic advection may be temporary in systems which admit flow instabilities, it is present during the evolution of the flow instability when the majority of mixing and reaction occur and so is highly relevant to these systems. In Section 6 we shall explore the effects of chaotic advection upon reaction stability and speciation in more detail.

5. Pore/fracture geometry and fluid mixing

5.1. Chaotic advection and dispersion at the pore-scale

The geometry of all open porous and fractured networks is inherently complex, and this complexity is further manifest in fluid transport. In this Section we explore the notion that such complexity is another mechanism by which efficient fluid mixing can occur from the viewpoint of chaotic advection. Although not widely recognized as such, chaotic advection arising from the complex geometry is responsible for hydrodynamic dispersion (Bear, 1972) in open networks, where the resultant dispersion is often several orders of magnitude greater than the underlying molecular diffusion.

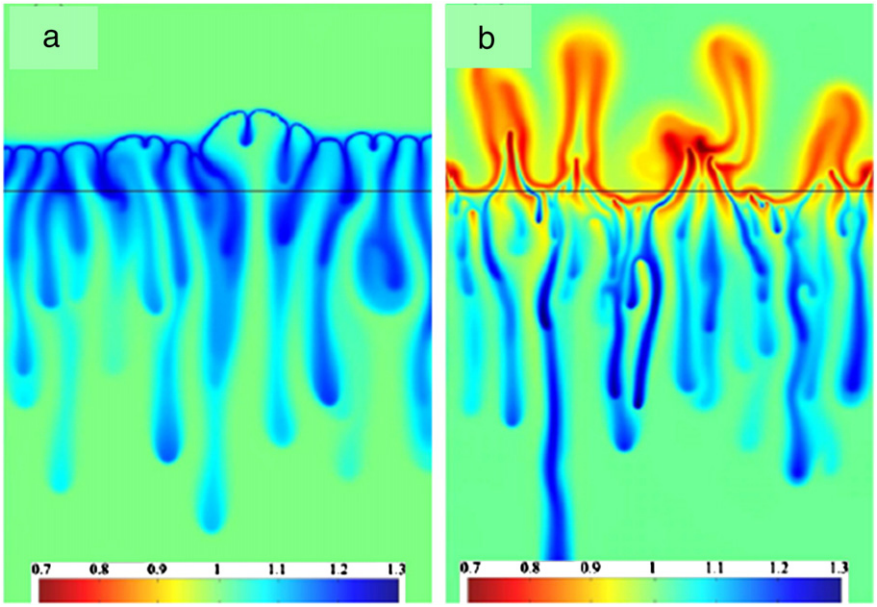

Fig. 4.6. Two dimensional density fields resulting solely from chemically driven hydrodynamic instabilities. The horizontal black line is the initial interface between a lighter fluid above and a denser fluid below. The chemical reaction $A+B\rightarrow C$ induces different patterns of behaviour depending on the values of the various parameters. For both cases $M_b=\delta_b=Da=d=1$. (a) $\delta_c=1$, $M_c=2.5$. Only Rayleigh–Taylor instabilities in C (blue) develop with upward convection. (b) $\delta_c=0.5$, $M_c=2.0$. Both Rayleigh–Taylor instabilites for C (blue) and upward rising plumes of A (orange) develop. The time is the same in both cases. For details see Almarcha et al. (2010).
After Almarcha et al. (2010).

Due to the inherent complexity of the pore-space, it is often convenient to model transport in open networks by averaging over many pore diameters, resulting in macroscopic equations for large-scale fluid flow coupled with dispersion models for large-scale transport. Typically, the averaged fluid flow equations are represented by Darcy's law, which has served well to capture the gross features of large-scale flow in open networks. However, in the process of averaging it is possible unwittingly to prohibit certain physical phenomena which may have significant implications for fluid mixing and transport. We shall explore this concept in greater detail throughout this Section.

As the Reynolds number for pore-scale flow is typically small, pore-scale fluid mechanics within the pore space Ω can be validly described by the incompressible Stokes equation

$$\mu\nabla^2\mathbf{v}-\nabla P=\mathbf{0},\ \nabla\cdot\mathbf{v}=0, \tag{5.1}$$

subject to non-slip conditions $\mathbf{v}|_{\partial\Omega}=0$ at the pore surface $\partial\Omega$. The complexity of the pore-space geometry means that a steady unidirectional pressure gradient can generate a steady 3D flow at the pore-scale which can exhibit chaotic advection via the advection Eq. (3.2). Chaotic advection in steady 3D flows has been exploited in the design of static mixers (Galaktionov et al., 2000; Singh et al., 2009); devices made of synthetic porous media are designed to maximise mixing during flow, as depicted in Fig. 5.1 (left). Fundamental to the operation of these devices are the actions of splitting, reorientation and recombination of fluid elements such that repeat actions create material distributions comprised of increasingly fine-scale striations, as shown in Fig. 5.1 (right) depicting evolution of the concentration distribution φ_n exiting the n-th mixing element.

The actions of fluid splitting and recombination also occur in all porous media with branching and merging pores. How pore branching and merging generate fine-scale structure is illustrated in Fig. 5.2, where the concentration field φ is split and recombined in a non-trivial way, eventually leading to complete mixing. Although this example represents a gross idealisation, the basic features of non-trivial pore branching and recombination is general to all but perfectly symmetric porous media (Carrière, 2007; Lester, submitted for publication; MacKay, 2001). In the case of multiple interacting pores the system is more complicated, but the underlying chaotic dynamics persist. Hence chaotic advection is inherent to all natural open porous and fractured networks.

Figs. 5.1 and 5.2 clearly show how chaotic advection at the pore-scale can significantly promote transverse dispersion (that is, dispersion transverse to the bulk flow direction) through accelerated

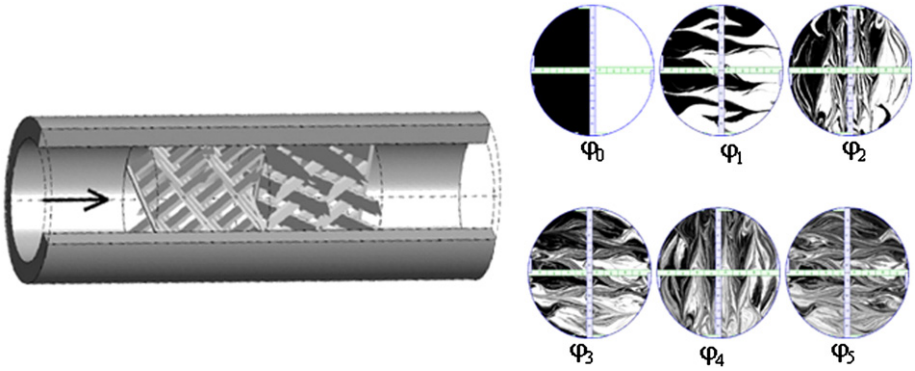

Fig. 5.1. Schematic of a static mixer, with bulk flow direction and several mixing elements shown (left). Evolution of the concentration field φ_n exiting the n-th mixing element (right).
After Singh et al. (2009).

mixing. Longitudinal dispersion (that is, dispersion parallel to the bulk flow direction) is related to the residence time distribution (RTD) of tracer particles flowing through porous media. In contrast to transverse dispersion, chaotic advection acts to suppress longitudinal dispersion due to the ergodicity of chaotic orbits, reducing the asymptotic scaling of RTD variance from t^2 to $t\ln(t)$ for non-diffusive tracers (Mezić, 1999). As such, chaotic advection has profound effects upon macroscopic transverse and longitudinal dispersion in porous media. As explored in Section 3, in conjunction with molecular diffusion, chaotic advection acts to accelerate dispersion exponentially. In the context of open porous and fractured networks, the phenomenon is manifest as hydrodynamic dispersion.

5.2. Chaotic advection and dispersion at the macro-scale

If we neglect the influence of gravity, flow in porous media at the macro-scale is described via Darcy's law, which relates the Darcy velocity $\hat{\mathbf{V}}$ to the gradient of the fluid pressure P via the permeability distribution $K(\mathbf{x})$ and the fluid viscosity μ as

$$\hat{\mathbf{V}} = -\frac{K(\boldsymbol{x})}{\mu}\nabla P \tag{5.2}$$

where the Darcy velocity $\hat{\mathbf{V}}$ is related to the pore-scale velocity $\mathbf{v}$ in Eq. (5.1) as $\hat{\mathbf{V}} = \varepsilon\langle\mathbf{v}\rangle$, where ϕ is the porosity, and $\langle\rangle$ denotes the averaging process. For heterogeneous media, the porosity ϕ and permeability $K(\boldsymbol{x})$ vary spatially, where the permeability is often modelled as a spatially correlated random function. As the correlation length-scale of K is much larger than the pore-scale, up-scaling is necessary to derive macroscopic transport equations (Neuman and Tartakovsky, 2009). Fluctuations in K generate fluctuations in the Darcy velocity $\hat{\mathbf{V}}$, and ensemble averaging of the transport equation is required to derive models of hydrodynamic dispersion.

For heterogeneous porous media, fluctuations in the permeability field K generate non-zero vorticity $\boldsymbol{\omega}$ in the Darcy flow as

$$\boldsymbol{\omega} \equiv \nabla \times \hat{\mathbf{V}} = -\frac{1}{\mu}\nabla K(\boldsymbol{x}) \times \nabla P. \tag{5.3}$$

Finite vorticity is a necessary ingredient for chaotic dynamics as steady irrotational flows cannot generate chaotic advection (Lester et al., 2009). However, Sposito (Garrison, 2001; Sposito, 1994) shows that although Darcy flow in heterogeneous systems is rotational, the flow helicity is identically zero

$$H := \int_{\Omega} \hat{\mathbf{V}}.\boldsymbol{\omega}\, d\Omega, \tag{5.4}$$

where the helicity, H, is a conserved quantity which measures the degree of knottedness of vortex lines (Moffatt, 1969), and is interpreted as an indicator of chaotic dynamics (MacKay, 2001). Hence, only 3D Stokes flow Eq. (5.1) can generate chaotic dynamics in steady flow in open porous networks, whilst the process of averaging to derive the Darcy flow Eq. (5.2) explicitly prohibits such phenomena.

However, *transient* Darcy flow, whether 2D or 3D, homogeneous or heterogeneous, can generate chaotic advection through flow reorientation and transient forcing (Jones and Aref, 1988; Lester et al., 2009; Trefry et al., 2012). Transient flow in hydrothermal systems can occur via a range of mechanisms such as flow instabilities, seasonal forcing and punctuated fluid infiltration (Miller and Nur, 2000). Studies of chaotic advection in transient potential flows (i.e. Darcy flow with homogeneous permeability) show that arbitrarily fine-scale filamentous structures can result from repeated stretching and folding motions brought about by transient forcing involving flow reorientation. Although the underlying flow field is irrotational, switching of forcing protocols for potential flows invokes flow reorientation, allowing the formation of structures (heteroclinic and homoclinic connections, Wiggins and Ottino, 2004) which underpin generation of chaotic advection. This behaviour persists for heterogeneous Darcy flow, although the rate of mixing is retarded in regions of very low permeability. Transient flow in hydrothermal systems can be driven by a variety of mechanisms (Cox, 1995; Cox and Ruming, 2004; Miller and Nur, 2000; Ord and Henley, 1997; Sibson, 1987, 2007) and the majority of these mechanisms admit flow reorientation and hence chaotic advection through cyclic forcing.

In conjunction with diffusion, such flows share many of the features of chaotic advection in general. Filamentous structures down to arbitrarily small length scales can be created by the flow, and diffusion acts to cut off this length scale via the smearing of fine-scale striations. Again this leads to the formation of strange eigenmodes (Eq. (3.5)) governing evolution of the concentration field, and exponential acceleration of dispersion rates is observed (Adrover et al., 2002a; Lester et al., 2008).

Along with the reaction-driven flow instabilities considered in Section 5, fluid flow in hydrothermal systems also gives rise to chaotic advection via two mechanisms over a wide range of length-scales. First, the geometry of open porous and fractured networks can generate chaotic advection through pore branching and recombination, where steady 3D Stokes flow within the pore-space captures the essential fluid dynamics. Secondly, at larger scales transient Darcy flow can give rise to chaotic advection via flow reorientation events which admit the building blocks of chaotic advection. We argue that the first mechanism is ubiquitous to all natural porous media, whilst the second arises through natural mechanisms (Cox, 1995; Miller and Nur, 2000; Ord and Henley, 1997; Sibson, 1987) which drive transient flow such as cyclic forcing and punctuated fluid infiltration. In both cases, the combination of molecular diffusion and chaotic advection in hydrothermal systems can generate exponentially accelerated dispersion, as is discussed in Section 3. Such dispersion acts to accelerate chemical reactions borne in the host fluid, but also the action of chaotic advection can profoundly alter the stability of chemical

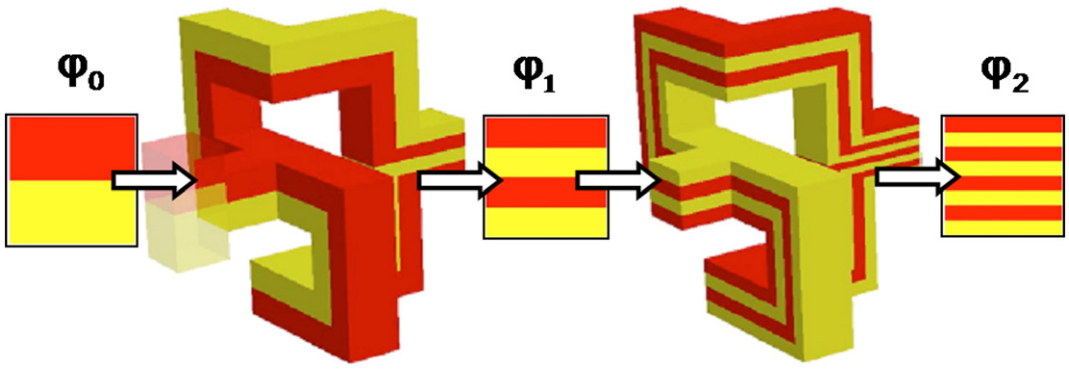

Fig. 5.2. Non-trivial pore branching and merging generates topological chaos and complete mixing. After Carrière (2007).

reactions relevant to mineralisation, and in turn modify the spatial distribution of mineral deposition.

6. Chaotic advection and chemical reactions

In this section we review the literature exploring the coupling between chaotic advection and non-equilibrium chemical reactions typical of hydrothermal systems. The important points that arise from such coupling are: (i) the mixing process produces a multifractal spatial distribution of constituents which arises from interwoven filaments of the mixing fluids, (ii) these filaments are continuously stretched and folded by the flow, (iii) the stretching significantly enhances chemical reaction rates, (iv) the mode of chemical reaction (stable, bistable, oscillatory, chaotic) is strongly influenced by the fractal geometry of the filaments. We explore these issues in the various sections below.

6.1. Background

As established in Sections 4 and 5, flow in porous media can generate chaotic advection through various mechanisms over a range of length-scales of several orders of magnitude, from the pore-scale to macroscopic flow on the scale of kilometres. Chaotic advection as such can lead to rapid dispersion of passive tracers toward the homogeneous well mixed state. However, when active chemical processes are present in these flows, the coupling of reaction and dispersion can generate heterogeneous concentration distributions of the constituent species which are not dispersed toward homogeneity unless the system reaches an equilibrium state. As discussed in Part I, non-equilibrium chemical reaction conditions can occur in hydrothermal systems when chemical reactants are continually fed to the reaction site, and this non-equilibrium state can be maintained indefinitely. Similarly, non-homogeneity of spatial concentration distributions can also be maintained indefinitely under these conditions. It is believed that such heterogeneous distribution gives rise to observations of mineral depositions which are multifractal, and are a result of the interplay of complex chemical kinetics with chaotic advection. For the case of chemical reaction, the constituent species are termed *active*, in that they react whilst being transported by the advective flow field and molecular diffusion, and so the nature of this transport plays an important organizing role in controlling the spatio-temporal template upon which the reactive dynamics play out.

We make the simplifying assumption in this Section that the flow field is independent of both the species concentrations and reaction dynamics. Clearly this assumption of one-way coupling between fluid flow and concentration distributions is not valid for reactive systems considered in Section 4 involving strong variations in fluid density, viscosity, surface tension or chemical potential which can drive fluid flow. Although these mechanisms represent physicochemical phenomena important to fluid transport and reaction, and the coupled physics (that is, consideration of, for example, Rayleigh–Taylor, Rayleigh–Bénard, Plateau–Rayleigh, Saffman–Taylor instabilities) must be considered to describe particular systems, for the sake of clarity we shall here only consider one-way coupling although the subject is worthy of considerable further study. The core result, that chaotic advection can fundamentally alter the qualitative behaviour of non-equilibrium chemical systems, still persists for two-way coupled flow and reaction systems, with the distinction that the flow field and hence chaotic dynamics cannot be specified a priori.

6.2. The advection–diffusion–reaction (ADR) systems

For one-way coupled systems, the transport mechanisms of advection and diffusion act as an organizing template upon which the chemical reaction dynamics are localised, and the properties of this template can strongly influence the reactive dynamics. We formalize these concepts by considering the advection–diffusion–reaction (ADR) system (2.1) describing the evolution in time of the spatial concentration distributions c_i of a set of i species undergoing coupled chemical reaction and fluid transport via advection and molecular diffusion. The Damköhler number Da_i of species i characterises the relative timescales of reaction rate k_i and advection

$$Da_i = \frac{k_i L}{v}. \tag{6.1}$$

Typical reaction rates for reactions relevant to mineral precipitation occur on the order of $k_i \sim 10^{-2}\ s^{-1}$, and so typical Damköhler numbers for reactions in microfractured porous media (where v may be 10^{-5} m s^{-1} and the pore size, L, is of order 10^{-3} m) are of order unity, $Da_i \sim 1$, suggesting advection and reaction occur on similar timescales. As typical Péclet numbers are of order $Pe_i \sim 10^3$, diffusion is slow, and so chaotic advection has a significant influence in accelerating dispersion in these systems.

6.2.1. Dynamics of simple reactions

For simple chemical reactions such as the bimolecular collision reaction $A + B \rightarrow C$, describing the irreversible reaction of species A and B to form product C, if the reaction rates and species diffusivities are symmetric, that is,

$$F_A = F_B, Da_A = Da_B, Pe_A = Pe_B \tag{6.2}$$

then the ADR (2.1) reduces to an advection–diffusion Eq. (3.4) under the change of variable $\varphi = c_A - c_B$. In this case the transport and reaction dynamics decouple, and spatial homogenization of the system is governed by mass transport whilst the reaction dynamics independently control evolution of the system toward chemical equilibrium. For closed flows, the concentration difference φ decays to a constant value

$$\varphi_\infty = c_{A,0} - c_{B,0}, \tag{6.3}$$

where $c_{i,0}$ is the average initial concentration of species i, irrespective of the reaction kinetics.

Although reaction kinetics may be fast or slow with respect to the time-scale of transport, in all cases accelerated dispersion as quantified by the strange eigenmode decay rate (3.5) acts to increase the observed rate of reaction. In the limit of fast reaction kinetics, i.e. $Da_i \rightarrow \infty$, the ADR system is mass-transfer limited, and the concentrations of reactive species closely approximate local equilibrium conditions $c_{i,e}$, given implicitly as

$$F_i\left(c_{1,e}, c_{2,e}, \ldots, c_{\kappa,e}\right) = 0, i = 1, \ldots, \kappa. \tag{6.4}$$

Under these conditions, the system is governed completely by the transport Eq. (3.4), the reaction kinetics is effectively instantaneous, and so the observed reaction rate scales directly as the dispersion rate in Eq. (3.5). Away from the limit of infinite reaction rates, the action of chaotic advection to create large inter-material surfaces to accelerate mass transfer and hence reaction (Adrover et al., 2002b; Arratia and Gollub, 2006; Berti et al., 2005; Cerbelli and Giona, 2009; Cerbelli et al., 2004, 2008; Lester et al., 2009; Tang and Boozer, 1996, 1999) still persists for systems with large but finite Da_i.

Toward the opposite limit of slow reaction dynamics, $Da_i \rightarrow 0$, the constituent species become well-mixed before reactions proceed. In this case the full ADR system reduces to that of a reactive system with well-mixed components

$$\frac{dc_i}{dt} = Da_i F_i(c_1, c_2, \ldots, c_I), i = 1, \ldots, I \tag{6.5}$$

and the reaction kinetics govern the full dynamics of the system. Note that fast transport dynamics not only corresponds to the parametric limits of vanishing Damköhler or Péclet numbers, but fast transport dynamics can also occur at finite Da_i and Pe_i if transport via chaotic advection is effective enough that the timescale of transport and reaction decouple. The exponential acceleration of transport in chaotic flows discussed above can engender this behaviour. Analytic solution of the system may be possible in this limit for simple forms of the coupled reaction kinetics, and the notion of heterogeneously distributed reactants breaks down.

6.2.2. Simplified models of the ADR system

The simplifications above illustrate the effects of chaotic advection on the rate of reaction in stirred fluid environments for particular dynamical regimes, with the universal behaviour that accelerated transport due to chaotic advection increases the reaction rate for simple reactions. However, for more complex reaction schemes involved in mineral precipitation, such as autocatalytic redox reactions, multistable nonlinear reactions and thermo-catalytic reactions, the impact of the chaotic advection template does not simply result in accelerated dynamics, but rather the complex interplay between reaction and chaotic advection can significantly alter the character of the reaction kinetics. These alterations can change the stability of reaction dynamics (Clifford et al. , 2000; Kiss et al., 2003a, 2004), alter state selection (Neufeld et al., 2002) and change the dynamics of species competition (Scheuring et al., 2003). It is these changes which result in profound changes to the evolution of chemical system dynamics which are wholly unexpected when considering chaotic advection as simply a means of accelerating transport and passive mixing.

As the complete numerical solution of the full ADR Eq. (2.1) for chaotic flows is often computationally expensive, many workers (Clifford et al., 1998, 2000; Cox, 2004; Cox and Gottwald, 2006; de Moura and Grebogi, 2004a, 2004b; Fields and Ottino, 1987a, 1987b, 1987c; Finn and Cox, 2011; Hernandez-Garcia and Lopez, 2004; Hillary and Bees, 2004; Karolyi and Tel, 2007; Karolyi et al., 1999, 2004; 2005; Kiss et al., 2003a, 2003b, 2004; Lopez and Hernandez-Garcia, 2002; Lopez et al., 2001; Martin, 2003; Menon and Gottwald, 2005, 2009; Muzzio and Liu, 1996; Muzzio and Ottino, 1989, 1990; Neufeld, 2001; Neufeld et al., 2002; Ottino, 1994; Pentek et al., 1999; Scheuring et al., 2003; Sokolov and Blumen, 1991a, 1991b, 1991c; Tel et al., 2000, 2005; Toroczkai et al., 2001; Tsang, 2009; Vollmer, 2002) have sought reduced models of the full dynamics, which also generate insights into the coupling between chaotic advection and reactive dynamics and lead to effective models which elucidate the impact of these couplings. Although these reduced models are often not quantitatively accurate representations of the full dynamics in certain dynamical regimes (particularly regions in the Pe–Da plane) they do reflect the governing dynamics and in certain instance act as quantitative proxies for the full dynamical system.

The most useful family of reduced models of the full ADR system are the lamellar (or Lagrangian filament) models which reduces the ADR system (2.1) in 2D domains to a 1D equation describing the evolution of component c_i. Chaotic flows create stretching and folding motions which produce filamentous striations at high Pe, and so reactions occur at the material interfaces defined by the filamentous structures. It is these filamentous structures which present difficulties for the full numerical simulation of the ADR system (2.1) as the resolution of many sharp interfaces throughout the fluid domain is numerically intensive. Conversely, the structure of the filamentous striations facilitates approximation of the system by taking a 1D slice along with coordinate $\boldsymbol{x}$ transverse to a local filament.

6.2.3. Chemical transitions induced by chaotic advection

Although reduced models do not necessarily capture all of the quantitative features of the full ADR system, they can be used to analyse reaction dynamics for other reaction schemes. Neufeld et al. (2002) consider the impacts of chaotic advection upon flows with multiple equilibrium states including autocatalytic and bistable reactions. The autocatalytic reaction $A+B\rightarrow 2B$ represents a simplified model of a wide range of reactive dynamics, including many relevant to mineral precipitation such as autocatalytic redox reactions and thermo-catalytic reactions. The reaction kinetics are

$$F_A = -F_B = k c_A c_B, \tag{6.6}$$

where c_A, c_B are the concentrations of species A and B. The reaction dynamics may be simplified via the proportion $c = c_B/(c_A + c_B)$, yielding

$$F_c = -k c(1-c), \tag{6.7}$$

and so there exist two equilibrium states; an unstable state at $c=0$ (no catalytic material) and a stable state at $c=1$ (all material catalysed). These kinetics result in a reaction front of the stable phase ($c=1$) penetrating into the unstable phase ($c=0$) which leads to fattening of striations of c in opposition to contraction due to chaotic stretching.

The reaction kinetics for the bistable model involves the species c_1

$$F_1 = k c_1(\alpha - c_1)(1-c_1) \tag{6.8}$$

which has two stable fixed points at $c_1=0$ and $c_1=1$, whose basins of attraction are separated by an unstable fixed point $c_1=\alpha$. Although this model does not represent an explicit chemical reaction *per se*, it is the simplest chemical scheme which represents multi-stability over the states $c_1=0, \alpha, 1$, and so is relevant to the reactions encountered in hydrothermal systems. If a perturbation away from a stable state $c_1=0$ or $c_1=1$ crosses the threshold values $c_1=\alpha$, then such perturbations propagate through the system, whereas smaller perturbations die out with time.

For closed flows, Neufeld et al. (2002) observe a critical Damköhler number Da_c for both chemical models which signifies a transition between equilibrium states at long times. For the autocatalytic reaction, an initially small perturbation around the unstable state $c=0$ dies out in the fast stirring regime $Da<Da_c$ as the transport dynamics homogenizes the perturbation too quickly for the unstable state to propagate (Fig. 6.1). Conversely, above Da_c, the initial localised perturbation grows to $c=1$ and propagates throughout the domain in the form of a filament of roughly constant width and exponentially growing length until the entire domain is filled with the stable state $c=1$. For the bistable reaction, localised perturbations also die out for $Da<Da_c$, but above Da_c the behaviour is dependent upon α. For $\alpha<0.5$, a global transition to $c=1$ occurs as per the autocatalytic case, but for $\alpha>0.5$, the localised perturbation decays. Similar results occur for an open flow, with the distinct difference that for $Da>Da_c$ the local perturbation produces a filament which is not space-filling (as this is incompatible with the boundary conditions) but rather the filament converges to a non-uniform stationary pattern which is in phase with the periodicity of the flow, as illustrated in Fig. 6.2.

Similar behaviour has been observed for more complex reaction processes, including combustion reactions (Kiss et al., 2003a), oscillatory chemical reactions (Kiss et al., 2004) and excitable media (Neufeld, 2001). These studies clearly demonstrate how chaotic advection can impart transitions for complex chemical reactions typical of hydrothermal systems. The actions of chaotic advection upon chemical and biological reaction extend beyond stability transitions; chaotic advection can also act to alter the character of chemical models.

6.3. Chaotic advection and reactions in open porous media flow

6.3.1. Properties of open flow systems

Fundamental differences between ADR systems posed in closed and open flow domains are exemplified by the long-term behaviour of the autocatalytic reactions as shown in Figs. 6.1(b) and 6.2(b). In closed domains, the zero-flux boundary conditions ensure that the

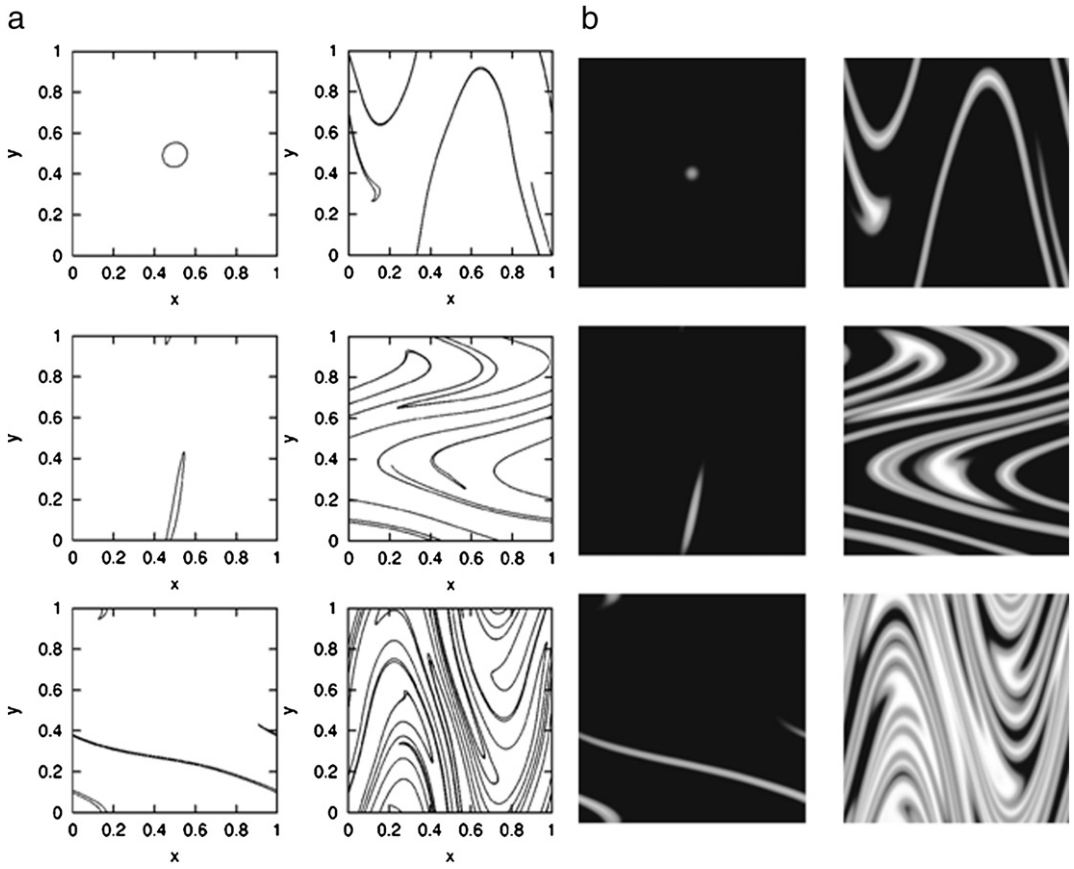

Fig. 6.1. (a) Temporal evolution of a material line advected by the closed flow. The radius of the initial circular contour is r = 0.06 and the figures correspond to t = 0.0, 0.5, 1.0, 1.5, 2.0, 2.5 (b) Snapshots of the spatial distribution for the autocatalytic reaction for Da = 1.0 ($<Da_c$) at t = 0.0, 2.0, 4.0, 6.0, 8.0. The amplitude of the initial perturbation is chosen to be $c_0 = 0.5$ in order to make the initial decay visible.
Reproduced from Neufeld et al. (2002).

finite amounts of reacting species eventually are driven to a homogeneous equilibrium state, as per Fig. 6.1(b). As there are no concentration gradients in the long-time limit, chaotic advection has no effect here and so general chaotic advection only acts on transient behaviour in closed systems. Conversely, the continual influx of reactants in open flows can indefinitely sustain spatio-temporal patterns and hence concentration gradients, as per Fig. 6.2(b), where the filamentous distribution of reactants in the autocatalytic model is maintained as a stationary pattern. As hydrothermal systems are typified by open flows with continual influx of reactants, henceforth we shall focus on the dynamics of chemical reactions relevant to mineralisation in open flows which admit chaotic advection.

Many workers have considered the influence of chaotic advection in open flows with complex chemical and biological reactions, ranging from plankton blooms in ocean currents (Hernandez-Garcia and Lopez, 2004; Hillary and Bees, 2004; Martin, 2003) and population dynamics (Lopez and Hernandez-Garcia, 2002; Lopez et al., 2001; Scheuring et al., 2003), through to blood coagulation (Pompano et al., 2008) and predator–prey systems (Karolyi et al., 1999). Various workers (Karolyi and Tel, 2007; Karolyi et al., 2004; Tel et al., 2000; Tel et al., 2005) have developed a theory of reaction dynamics in open chaotic flows which is based on a combination of bandwidth dynamics for the filamentous structures (a form of lamellar modelling) and discrete modelling of reactive particles. We review the main results of this theory and translate these outcomes into implications for a range of chemical reaction models relevant to mineral precipitation.

Given the assumption of one-way coupling between the advection and reaction dynamics, it is instructive first to consider the effects of open chaotic advection on passive particles to develop an overview of the organizing template imparted by the open flow field. For simplicity of exposition we shall initially consider coupled ADR systems in open 2D flows which exhibit chaotic advection. Although this geometric idealisation is not relevant to open porous and fractured networks, the fundamental concepts and basic results of ADR systems in 2D flows extend to 3D flows with only minor variations. We shall consider this extension in Section 6.3.5.

In open flows, chaotic regions of the flow contain a fractal set of non-escaping orbits, which correspond to the periodic points of the chaotic region. This set of zero measure (i.e. it is comprised of fluid particle orbits which have zero volume) is called the *chaotic saddle*, and this set controls transport in the flow. Associated with the chaotic saddle is the *stable manifold* which is a set of fluid particle orbits (also of measure zero) which approach the chaotic saddle asymptotically closely with increasing time $t \to \infty$ and never leave the chaotic saddle. In this sense, the stable manifold is *attracted* to the chaotic saddle and particles exactly on the stable manifold remain there for all time. Particles near to the stable manifold remain in the chaotic saddle for long times (which increase with proximity to the stable manifold) but eventually leave the saddle and are swept downstream.

Conversely, the *unstable manifold* is associated with the set of particles which move asymptotically close to the chaotic saddle with *decreasing* time $t \to -\infty$, such that the unstable manifold is *repelled* by the chaotic saddle, and points exiting the chaotic saddle are near to the unstable manifold. Hence the unstable manifold can be indirectly visualized in dye-trace experiments (Metcalfe et al., 2010a, 2010b) as the striations leaving the chaotic region into the regular flow, as shown schematically in Fig. 6.3. It turns out that the geometry of these manifolds has a direct influence on the overall system dynamics once chemical reactivity is introduced into the process.

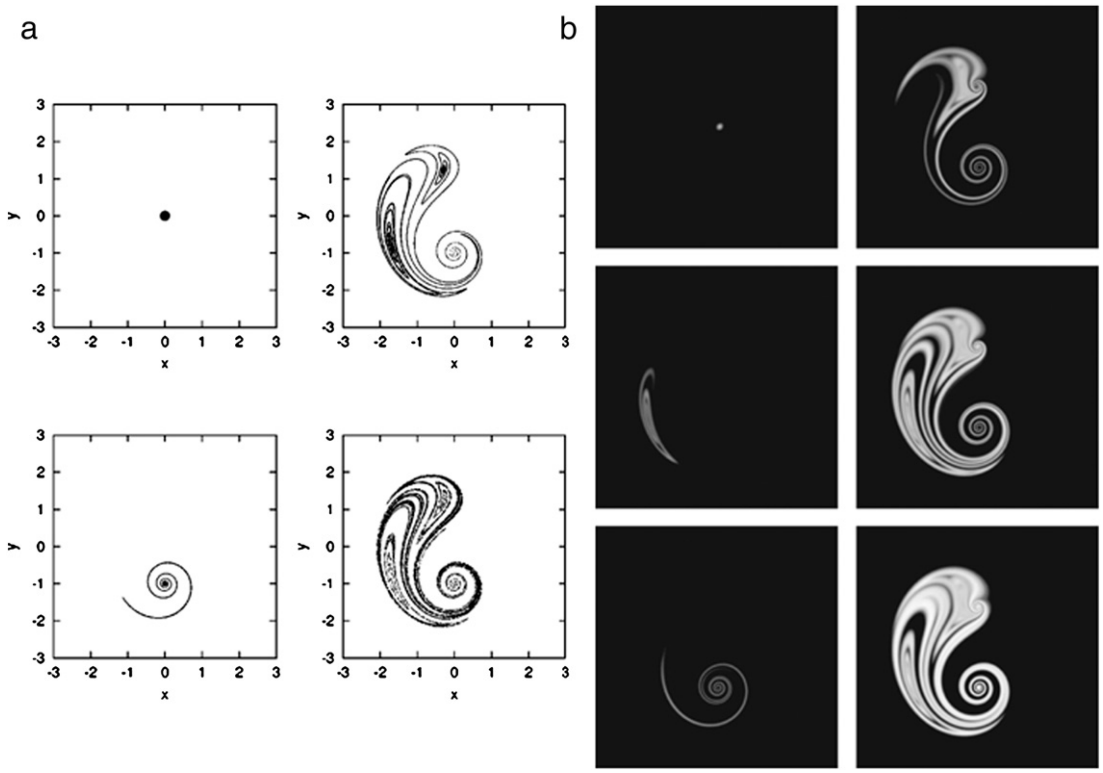

Fig. 6.2. (a) The evolution of an ensemble of particles (e.g., representing a droplet of dye) in the open flow system (t = 0.0, 2.0, 4.0, 6.0); (b) snapshots of the spatial distribution for the autocatalytic reaction in the open flow system for a supercritical Damköhler number, Da = 14.0 ($>Da_c$) at t = 0.0, 1.0, 2.0, 3.0, 4.0, 5.0. The distribution at t = 5.0 has already reached the time-periodic stationary state. The amplitude of the perturbation is $c_0 = 0.5$. For subcritical Damköhler numbers the perturbation dies out. (The bistable model shows similar behaviour but for different values of Da.)
Reproduced from Neufeld et al. (2002).

This result reflects the one-way coupling of the advection and reaction dynamics: the unstable manifold is the organizing structure which dictates how material leaves the chaotic saddle. It is also this organizing structure which dictates the distribution and geometry of filamentous structures and material distributions, and it is at the boundaries of these structures where reactions typically occur. Hence the unstable manifold is the organizing template upon which reactive dynamics evolve, with the subtle but important difference that the unstable manifold is an object of zero volume, whilst the reaction dynamics play out along the boundaries of filamentous structures which represent a "fattened-up" unstable manifold with positive volume. Significant insights into mineralisation reactions in open flows can be gleaned by considering the geometry of these fractal filaments.

The chaotic dynamics in open flows may be classified as either hyperbolic or non-hyperbolic (Wiggins and Ottino, 2004), the latter case identified by the presence of regular *islands* (Section 3) in the chaotic saddle. For hyperbolic systems, the fractal dimension D_f of the chaotic saddle is related to the escape rate κ and Lyapunov exponent λ as

$$D_f \approx 2 - \kappa\lambda, \tag{6.9}$$

where the number of particles trapped in the chaotic saddle decays as $\exp(-\kappa t)$. Although the fractal dimension D_f is a purely geometric measure, this quantity has a profound effect upon the reaction dynamics. For non-hyperbolic systems, regular islands or *KAM tori* (Ottino, 1989) can occur within the chaotic saddle and represent barriers to transport. As such, fluid trajectories initially outside the chaotic saddle only sample the unstable part of the saddle, which can alter the dynamics of the coupled ADR system. It is anticipated that hydrothermal systems admit both hyperbolic and non-hyperbolic open flows, however for simplicity of exposition we shall initially focus on hyperbolic systems, with extension to non-hyperbolic flow treated explicitly in Section 6.3.6.

6.3.2. Autocatalysis in open flows

Fig. 6.4 shows the results of a 2D particle-based numerical simulation for the autocatalytic reaction (6.6) in a time-periodic vortex shedding flow around a cylinder, where the B-particles are shown in black against a solution containing a high concentration of A-particles (not shown). A seed of B-particles is introduced upstream of the cylinder, which is quickly stretched and folded into a filamentous structure in the chaotic region in the cylinder wake. These filaments are continuously fattened due to reactive fronts moving out transverse to the stretching direction, and B-particles are continuously swept downstream by trajectories escaping the chaotic saddle. These processes balance within a few flow periods, and so the distribution of B-particles converges to stationary filamentous pattern which persists for arbitrarily long times. For different initial conditions the system evolves to the same stationary pattern, so long as the seed blob of B-particles enters the chaotic saddle, regardless of its size.

Although the vortex shedding flow is unlikely to occur in hydrothermal systems, the relevant properties of this flow (i.e. an open flow which admits chaotic advection) can occur in hydrothermal systems (as established in Sections 5 and 6), and so the general properties of the ADR system in Fig. 6.4 are representative of autocatalytic reactions in hydrothermal systems. The 1D Lagrangian filament model for the autocatalytic chemical model is of the form

$$\frac{\partial c}{\partial t} - \lambda x \frac{\partial c}{\partial x} = \frac{1}{Pe}\frac{\partial^2 c}{\partial x^2} + Da\, c(1-c), \tag{6.10}$$

where x is the coordinate transverse to the filament, and the convection term $-\lambda x.\, \partial c/\partial x$ represents stretching of the filament proportional

to the Lyapunov exponent λ. As such, the width δ of filament of B-particles evolves as

$$\frac{d\delta}{dt} = -\lambda\delta + 2\nu, \tag{6.11}$$

where ν is the velocity of the propagating reaction front which is dependent upon the autocatalytic reaction kinetics (6.7) and diffusivity D as

$$\nu = 2\sqrt{kD}. \tag{6.12}$$

Hence the filament width evolves to the steady state $\delta = 2\nu/\lambda$, as shown in Fig. 6.5. Consideration of these dynamics on the unstable manifold leads to an augmented rate equation for the production of the total number N_B of species B in the chaotic saddle of the form

$$\frac{dN_B}{dt} = -\kappa N_B + q\kappa\frac{\nu}{\lambda}N_B^{-\beta} \tag{6.13}$$

where q is a dimensionless geometrical factor and β is a constant solely dependent upon the fractal dimension D_f,

$$\beta = \frac{D_f - 1}{2 - D_f}. \tag{6.14}$$

The term $-\kappa N_B$ in Eq. (6.13) represents outflow of species B from the chaotic saddle, and the latter term represents production of B due to the autocatalytic reaction. As $1<D_f<2$, β is always positive, and so the production of species B *increases* with *decreasing* N_B, diverging as $N_B \to 0$. The appearance of a negative exponent in Eq. (6.13) markedly alters the reaction dynamics, leading to *singularly enhanced productivity* for the autocatalytic species B. Such behaviour is a general property of processes on fractal filaments with $1<D_f<2$, because the perimeter length of the filaments (where reaction occurs) increases as the area coverage decreases. These results indicate that the autocatalytic reactions which are important to mineralisation in hydrothermal systems are singularly stable for open flows which admit chaotic

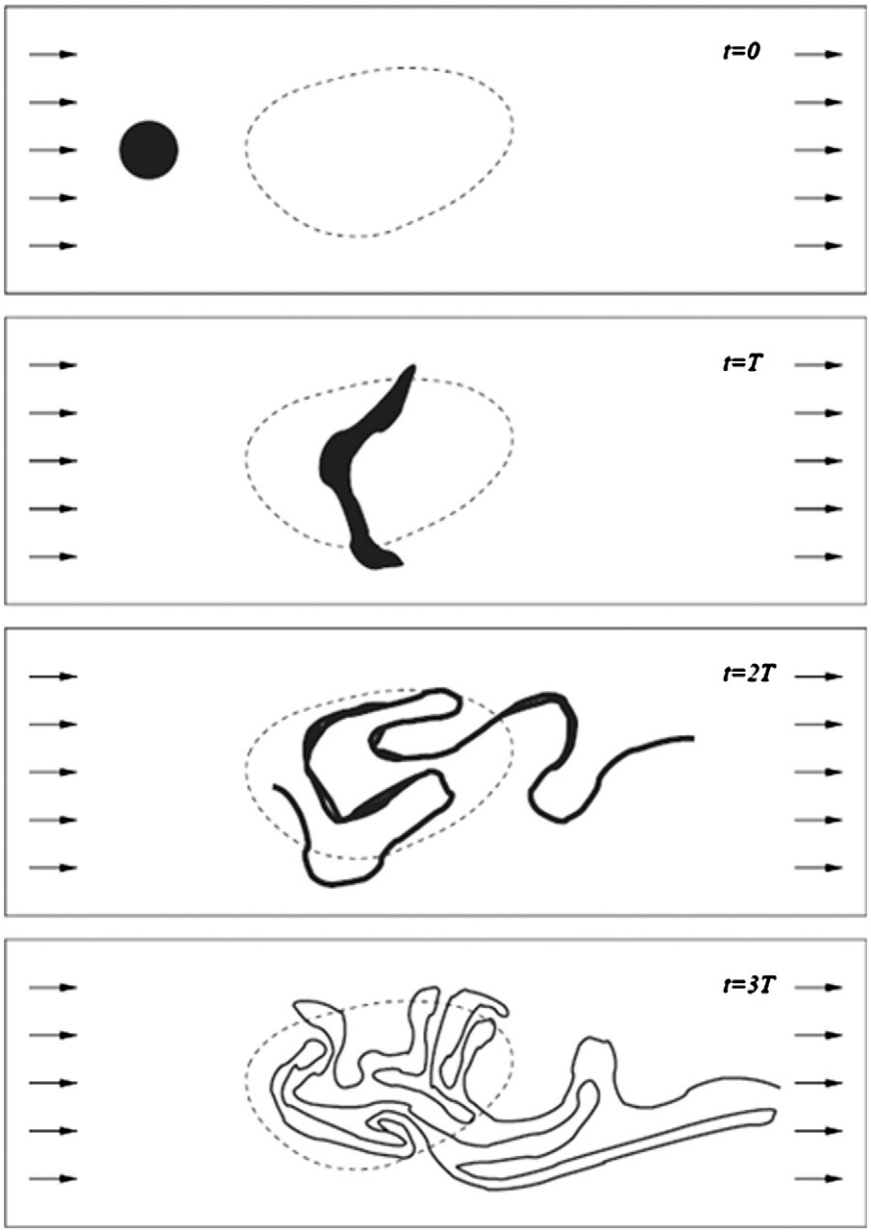

Fig. 6.3. Relevance of the unstable manifold: schematic diagram illustrating the distribution of an originally compact and small dye droplet in the mixing region of an open flow. After some time, the not yet escaped dye particles trace out the unstable manifold of the chaotic saddle existent in the mixing region. Reproduced from Tel et al. (2005).

advection. As we have established the propensity for open chaotic flows to occur in hydrothermal systems in Sections 4 and 5, then the results of Eq. (6.13) indicate that autocatalysis persists in these systems over a wide range of conditions and length-scales (Karolyi et al., 2004).

6.3.3. Competitive autocatalytic reactions in open flows

Such singularly enhanced behaviour also occurs for competitive reaction dynamics whereby two chemical species B_1 and B_2 react at different rates with species C according to the competing autocatalytic schemes $B_1 + C \rightarrow 2B_1$, $B_2 + C \rightarrow 2B_2$, as quantified by the coupled scheme for the concentrations c_{B1}, c_{B2}, and c_C:

$$F_{B1} = \alpha_1 c_{B1} - \mu_1 c_{B1}, \tag{6.15}$$

$$F_{B2} = \alpha_2 c_{B2} - \mu_2 c_{B2}, \tag{6.16}$$

$$F_C = -\alpha_1 c_{B1} - \alpha_2 c_{B2}, \tag{6.17}$$

where α_i and μ_i respectively are the formation and dissociation rates of species B_i which depend on the concentration of species C. Often the formation and dissociation rates of competing species will be imbalanced, and so in a perfectly mixed environment, direct analysis of the rate Eqs. (6.15)–(6.17) predicts extinction of the least competitive species, regardless of the form of the dependencies of μ_i and α_i on c_C. However, in imperfectly mixed environments, it is observed that the number of persistent species (i.e. B_1, B_2) greatly exceeds the number of limiting factors (i.e. C), in contrast to predictions made by the kinetics alone. This is exemplified by the so-called *paradox of plankton*, where the number of phytoplankton species stirred imperfectly by ocean currents exceeds the number of growth-limiting factors (Hernandez-Garcia and Lopez, 2004; Karolyi et al., 1999; Scheuring et al., 2003). This paradox may again be explained by the singularly enhanced production rate in the augmented reaction equations for dynamics on filamentary fractals

$$\frac{dN_{Bi}}{dt} = -\kappa N_{Bi} + q(D_f - 1)\frac{v}{L}N_B^{-\beta-1}N_{Bi} + q\frac{v_i}{L}N_B^{-\beta}p_i\left(\frac{N_{B1}}{N_{B2}}\right), i = 1, 2, \tag{6.18}$$

where $N_B = N_{B1} + N_{B2}$, and v_i, p_i respectively are the velocity of species B_i and the probability of species B_i being on the outside of a filament. Stability analysis (Scheuring et al., 2003) of Eq. (6.18) demonstrates that stable coexistence of species B_1, B_2 can occur in open flows which exhibit chaotic advection. This is illustrated in Fig. 6.6, which shows the steady state population distribution of two competitive species in

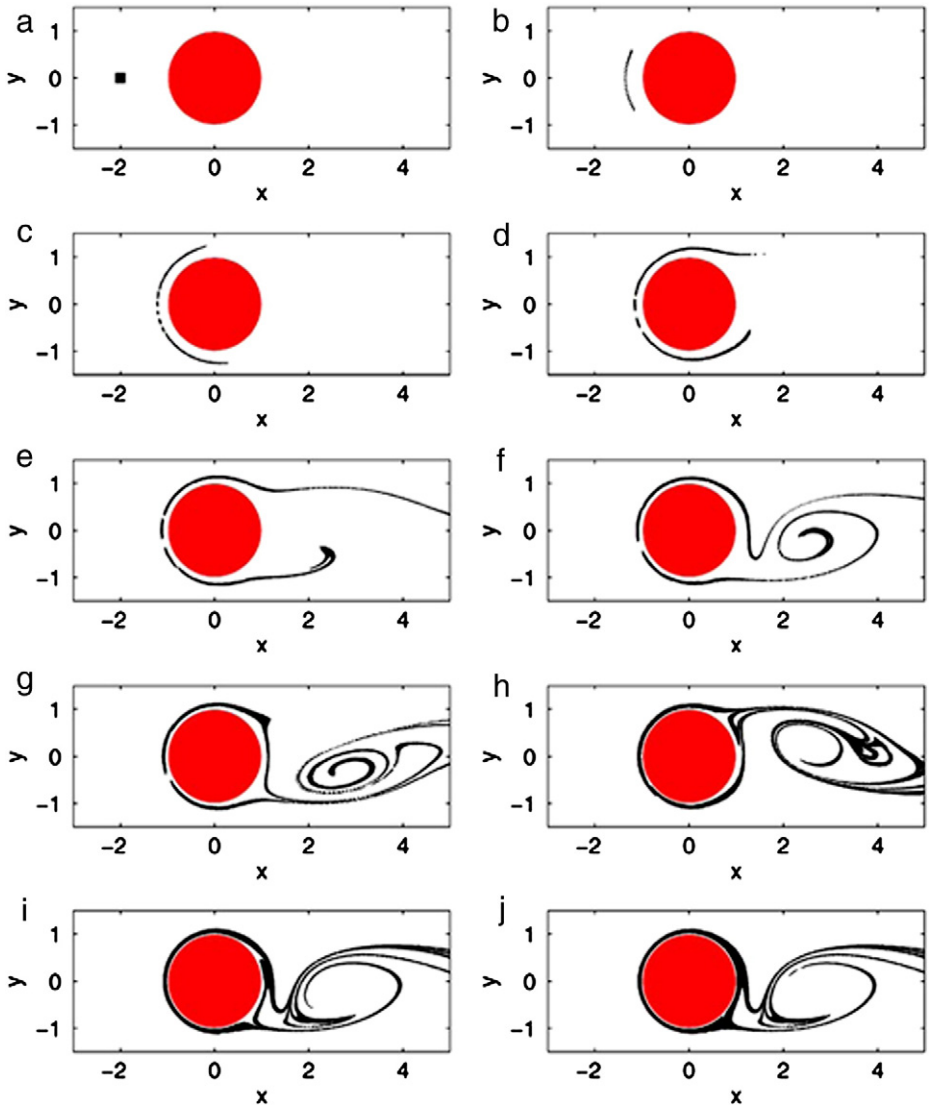

Fig. 6.4. Time evolution of a blob of *B* particles (black), initially placed close to the cylinder, interacting auto-catalytically with the surrounding *A* particles (white). The snapshots (a–j) are taken at times t = 0, 0.2, 0.4, 0.6, 0.8, 1.0, 1.2, 1.6, 2.0, and 3.0, respectively, right before a reaction takes place. ($t = 1$ is the period of the flow.) Reproduced from Tel et al. (2005).

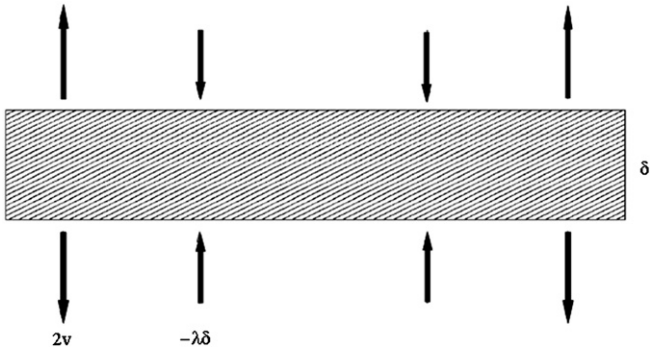

Fig. 6.5. Schematic diagram indicating the bandwidth dynamics: there is contraction across the unstable manifold due to the flow, and increase of the bandwidth due to reactivity.
Reproduced from Tel et al. (2005).

the wake of a von Kármán vortex street behind a cylinder. These results also extend to more complex metabolic models including cyclic competition (Karolyi et al., 2005) and metabolic activity (Karolyi et al., 1999). Although metabolic reactions and biological systems appear to share little in common with mineralisation in hydrothermal systems, the essential features of competing autocatalytic reactions are common to both systems. As such, the fundamental result that chaotic advection in open flows significantly promotes stable coexistence of competing autocatalytic species is highly relevant to hydrothermal systems. Eq. (6.18) suggests that such competing species are singularly enhanced (that is, their production increases without bound as their total concentration falls to zero) in a similar fashion to a single autocatalytic reaction (6.13). This result means that hydrothermal systems can support a wide range of competing autocatalytic species and so maintain chemical complexity as the mineralisation process evolves.

6.3.4. Bistable reactions in open flows

Along with autocatalytic reactions, reactions with multiple stable equilibria are important to hydrothermal systems (Sections 6 and 7, Part I). State selection or chemical speciation in such reactions is reflected in the mineral deposition process, and so it is important to understand how multi-stable reactions behave in flows which admit chaotic advection. The simplest form of multi-stable reaction is the bistable reaction (6.8) which possesses stable fixed points at $c_1 = 0$, $c_1 = 1$, and an unstable fixed point at $c_1 = \alpha$. For the bistable kinetics perturbations less than α do not persist, but larger ones grow to the stable limit $c_1 = 1$, and in this regime the dynamics share the same features as the autocatalytic reaction (6.7), yielding reactive fronts with velocity v proportional to $\sqrt{\mathrm{Pe}}$, and so singularly enhanced reaction kinetics (6.13) persist for bistable kinetics also (Neufeld et al., 2002). The major qualitative difference between bistable and autocatalytic dynamics in open flows is that the emptying transition at critical Damköhler number Da_c is of first order in the bistable case.

These results extend to reactions with multiple stable equilibria, where all of the stable fixed points of the chemical system experience singular enhancement due to the negative exponent in for example Eq. (6.13). As such, chaotic advection in hydrothermal systems promotes the coexistence of stable species through the same singular enhancement mechanism.

6.3.5. Reactions in 3D open flows

So far in this Section we have focussed on dynamics of ADR systems in 2D stirred open flows which possess one stable and one unstable manifold. These results for 2D systems may be extended to 3D flows, where there now exist 3 manifolds associated with the flow, which is assumed to be volume-preserving. As such the stretch rate of each manifold must sum to zero (to preserve volume), and so there exist two possibilities for the advection dynamics, depending on whether there exist two unstable and one stable manifolds (Type I) or one unstable and two stable manifolds (Type II), as per Fig. 6.7. For these flow types, with symmetric stretching (i.e. the stretch rate of the two unstable (stable) manifolds for Type I (Type II) flows is equivalent) the Lagrangian slice reaction kinetics are the same as for 2D flows (Eq. (6.14)) with the exponent β replaced by the 3D analogue β_{3D} (de Moura and Grebogi, 2004a, 2004b);

$$\beta_{3D} = \frac{D_u - 2}{3 - D_u} \tag{6.19}$$

where D_u is the fractal dimension of the unstable manifold which satisfies $1 < D_u < 3$. The major qualitative difference between 2D and 3D flows is that β_{3D} may be positive or negative, with $\beta_{3D} > 0$ for $D_u < 2$ and $\beta_{3D} < 0$ for $D_u > 2$. In contrast, for 2D flows $\beta > 0$ always occurs, giving rise to singularly enhanced production dynamics. The case $\beta_{3D} < 0$ may only occur in Type I flows, and the Lagrangian filament dynamics are no longer singular as the exponent $-\beta_{3D}$ is now positive. As such, in this case as N_B approaches zero, the production rate also approaches zero as per regular reaction kinetics. The transition between positive and negative β_{3D} appears to be associated with the transition point between smooth and fractal scattering behaviour of the advection dynamics for the underlying flow field. In terms of flow within hydrothermal systems, it is difficult to specify a priori whether the unstable manifold fractal dimension D_u for Type I flows is greater or less than the threshold value of 2, and this represents an important area of future research.

6.3.6. Reactions in non-hyperbolic open flows

For simplicity of exposition, so far in this Section we have assumed the open flow in hydrothermal systems to be hyperbolic — that is, no regular islands exist in the chaotic saddle. Non-hyperbolic flows contain regular islands or *KAM tori* (Wiggins and Ottino, 2004) which do

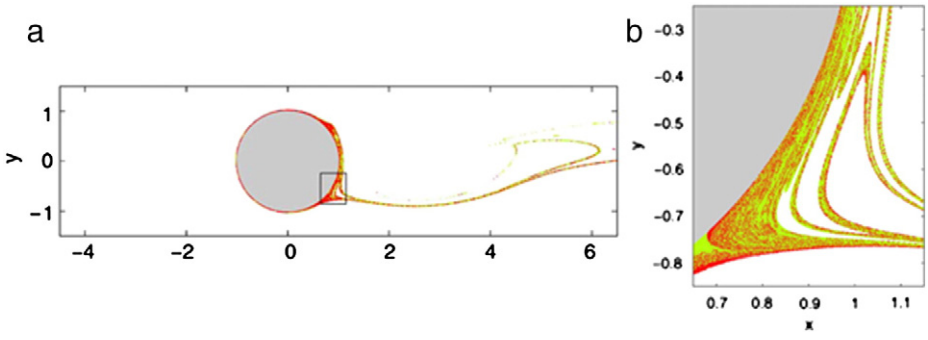

Fig. 6.6. Coexistence of two species in the von Kármán vortex street flow behind a cylinder. The figure shows a snapshot of the population distribution after steady state has been reached. The two species are green *B*1 and red *B*2.
Reproduced from Tel et al. (2005).

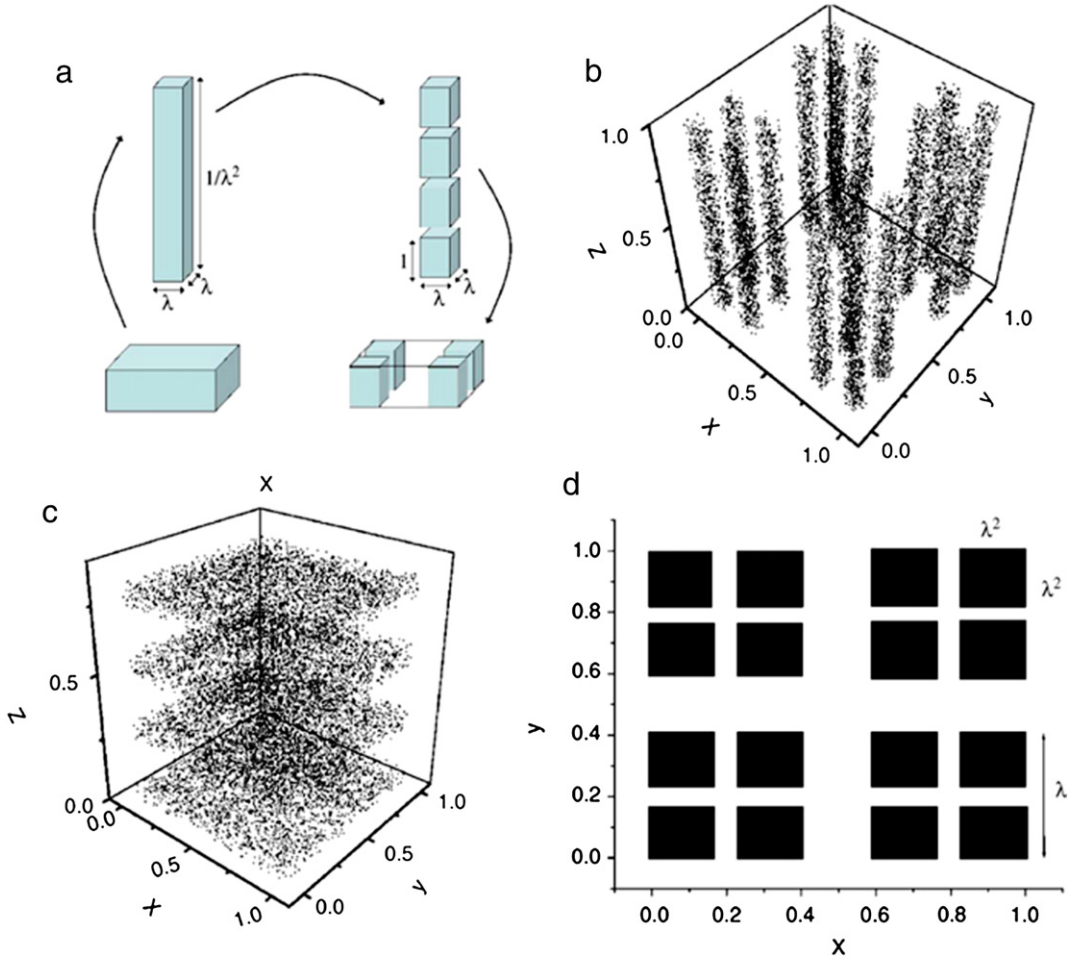

Fig. 6.7. (a) Illustration of the action of one iteration of map M on a cube of side L = 1 (Type I dynamics). The drawing is not to scale. (b) Surviving points after 2 iterations of the map M, for $\lambda = 0.35$, with initial conditions chosen randomly in the cube. (c) The same as (a), but for the inverse map $M-1$ (Type II dynamics). (d) Intersection with a horizontal plane (z = const.) of the set of surviving points after 2 iterations of M, with $\lambda = 0.35$.
Reproduced from Tel et al. (2005).

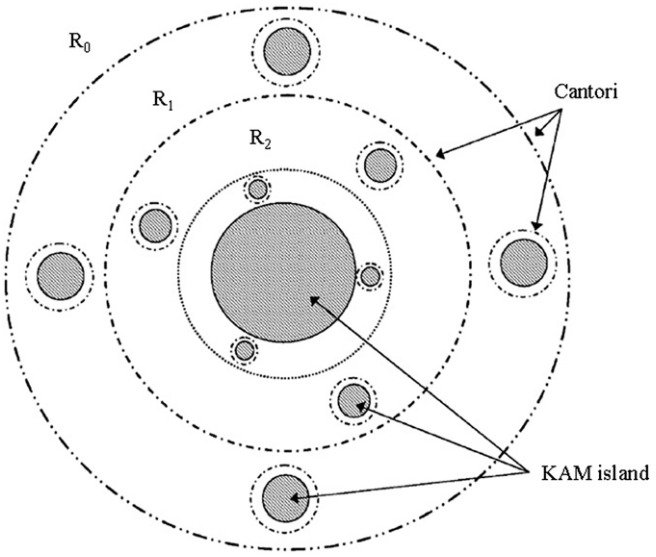

Fig. 6.8. Schematic illustration of the hierarchical structure of KAM islands and Cantori, generic in non-hyperbolic flows. Solid circles represent KAM tori, and Cantori are represented by circles with "gaps". R_i denotes a region belonging to level i in the hierarchy of Cantori.
Reproduced from Tel et al. (2005).

not exchange material with the surrounding fluid through separation via kinematic barriers. These islands occur as nested hierarchical structures with surrounding fractal structures called *cantori*, which are "leaky" invariant sets. These cantori act as partial barriers to transport, where material may be exchanged with the surrounding hyperbolic sea, although transport within the cantori is slow, on a diffusive time-scale, as illustrated in the schematic in Fig. 6.8. Several workers (de Moura and Grebogi, 2004b; Tel et al., 2005) have used the effective fractal dimension D_{eff} to characterise transport and reaction in non-hyperbolic systems, based upon extension of the usual fractal dimension D_f of the stable manifold in open chaotic systems defined as

$$D_{eff} = -\lim_{\varepsilon \to 0} \frac{\ln(N(\varepsilon))}{\ln(\varepsilon)}, \tag{6.20}$$

where $N(\varepsilon)$ is the number of boxes of size ε required to cover the stable manifold, with $1 < D_{eff} < 2$ for 2D systems. For non-hyperbolic systems, D_{eff} always assumes the maximum value of 2. The limit (6.20) is slowly convergent, and very small ε_{min} is required accurately to approximate the true limit. For finite resolution $\varepsilon > \varepsilon_{min}$, the effective dimension $D_{eff}(\varepsilon)$ is

$$D_{eff}(\varepsilon) = -\frac{d\ln(N(\varepsilon))}{d\ln(\varepsilon)}, \tag{6.21}$$

which is approximately constant over large ranges of ε. It transpires that the effective rate equation from the Lagrangian filament slice

model (6.13) which contains the singular enhancement production term describes reactions in non-hyperbolic systems, where the effective fractal dimension D_{eff} replaces D_f at a resolution corresponding to the reactive scale $\delta = 2\nu/\lambda$. This is directly invoked in the expression (6.14) for the exponent β. As such, although the transport dynamics of non-hyperbolic systems are qualitatively distinct from hyperbolic systems, the augmented rate Eq. (6.13) still describes the reaction dynamics as a singularly enhanced process with the only quantitative change of $D_{eff}(\varepsilon)$ replacing the fractal dimension D_f.

6.4. Implications for hydrothermal systems

In Sections 4 and 5 the propensity for chaotic advection to occur in hydrothermal systems via a variety of mechanisms was established. The results in this Section suggest that the presence of chaotic advection in hydrothermal systems has a significant impact upon the qualitative nature of the chemical reactions which lead to mineral deposition. A fundamental property of hydrothermal systems is that they are *open*, in that fresh fluid and chemical reagents can flow into the reaction site, and so the relevant chemical reactions can be maintained indefinitely in a state far from equilibrium. In conjunction with non-equilibrium chemistry, the open nature of the fluid flow also means that from the perspective of a fluid particle flowing through the system, chaotic advection is transient in that there exists a so-called chaotic saddle in which the particle resides for some time before exiting and moving downstream. Clearly the chaotic saddle may be very large for hydrothermal systems (perhaps as large as the system itself), the important point is that whilst a fluid particle is undergoing chaotic motion within the saddle there is an average flux in the bulk flow direction. The open nature of this flow and the continual feed of chemical reagents promote the formation of chemical distributions as fractal filaments which represent the unstable manifold of the flow which is "fattened-up" by diffusion and reaction. Chemical reactions occur at the interface of these filaments, and the fractal geometry of these structures has significant impacts upon the overall reaction dynamics.

Chiefly, the fractal nature of these filaments means that they have a large ratio of interfacial area to internal volume which increases to infinity as the filament thins (as the unstable manifold itself is fractal). As such, chemical species which are distributed fractally exhibit *singularly enhanced production rates* as their total mass goes to zero and as the relative rate of reaction at the filament interface grows without bound. Such singular production enhancement arises from the geometry of the unstable manifold only, and so appears to be *universal* with respect to chemical kinetics. As such, these concepts apply to a wide range of reactions relevant to mineralisation in hydrothermal systems, including autocatalytic reactions, multi-stable reactions, competitive reactions and reactions representative of excitable media involving catalysis (including thermal-catalysis) and inhibition. Such complex non-equilibrium reactions are of principal importance to mineral deposition, and the impact of singular production enhancement upon the persistence of particular species is profound. For instance, Henley and Berger (2000) have suggested the following set of reactions for the deposition of gold:

$$Fe^{2+}(aq) + H_2S \rightarrow FeS^* + 2H^+$$

$$FeS^* + H_2S \rightarrow FeS_2 + 2H$$

$$Au^+ + H \rightarrow Au + H^+.$$

These involve exothermic behaviour and hence can lead to unstable behaviour in an open flow system. The set of reactions is ideally suited for the development of singularly enhanced production of gold and pyrite in open vein systems and breccias with chaotic flow. By such a mechanism the deposition site stays fixed in space whilst the fluid passes by and precipitates gold and pyrite at enhanced rates so long as the Fe^{2+} in solution and H_2S are supplied. Coupled with the episodic precipitation of quartz and adularia or of quartz and chlorite/carbon arising from autocatalysis described in Section 7 of Part I the ubiquitous association of very high concentrations of gold and pyrite in quartz veins in epigenetic and orogenic gold deposits finds a compelling mechanism. It is important to note that identical mechanisms of enhancing the performance of open packed bed and fluidised bed reactors are widely recognized (Iordanidis et al., 2004; Van den Bleek and Schouten, 1993). In terms of linking such behaviour with spatial patterning of mineral deposits, the fractal distribution of the reaction sites (at the filament interface) renders mineral precipitation in such systems also to be fractally distributed, as is observed in the field. We shall explore these concepts in greater detail in Sections 7 and 8.

7. Discussion

Hydrothermal mineralising systems can be regarded as complex coupled advection–diffusion–reaction (ADR) systems involving multiple chemical species which react to form mineral deposits. Field observations of such deposits show complex spatio-temporal patterning over a wide range of length scales, from the grain scale to hundreds of kilometres. The challenge of these systems is to understand the complex array of coupled physical and chemical phenomena which lead to such deposition signatures, in order to improve our comprehension of observations and predict where viable deposits might occur. As such, it is instructive to consider: (i) what physico-chemical phenomena may occur in hydrothermal systems; (ii) what effects such phenomena have upon the mineralisation process; and (iii) how such phenomena may affect spatio-temporal patterning of mineral deposition. The two papers (I and II) in this series attempt to make some preliminary steps toward answering these questions, with an ultimate view of better understanding mineralisation events and supplying improved targeting criteria.

A characteristic property of such hydrothermal systems is that they are *open*, in that energy and mass may flow through the system due to the continual flux of heat, fluid and soluble chemical species. Such influx of chemical reagents can drive and maintain the system well away from equilibrium, and so traditional analyses of hydrothermal mineralising systems under the assumptions of chemical equilibrium are of limited applicability. Furthermore, the continual flow within these systems renders the coupled transport and reaction dynamics complex, and often simplifying assumptions of well-mixed concentration distributions are not valid. In Part I of this series we considered the range of complex chemical behaviour which reactions relevant to the mineralisation process can exhibit both with and without coupling to transport phenomena, such as oscillatory, chaotic, multistable and catalytic reaction kinetics. Part I corresponds to the assumption of well-mixed chemical constituents such that no spatial concentration gradients occur prior to chemical reactions taking place and so the spatial dimensions of the problem are not relevant.

However, it is recognized that hydrothermal systems are typically not well-mixed, and the relevant chemical species can exhibit strong spatial concentration gradients, such that reactions are often localised to reaction fronts at the interface between two chemical species. As such, fluid mixing plays an important role in the evolution of these coupled non-equilibrium ADR systems, and such dynamics must be considered in order to comprehend the process of mineral deposition. This is the role of the current paper in this series. In contrast to well-mixed species (those which posses homogeneous concentration distributions), simultaneous fluid mixing and reaction involve partially mixed constituents with very different concentration distributions (that is, highly striated, complex filaments) to that of the well-mixed state. As such, in the presence of chemical reaction, "partial" fluid

mixing generates very different behaviour than the two extremes of no mixing or complete mixing.

Fluid mixing as a fundamental ingredient of hydrothermal open flow systems can be achieved via several mechanisms. The natural language to understand and describe fluid mixing is that of dynamical systems, where the notion of so-called *chaotic advection* describes how fluid motion generates efficient mixing through iterated fluid stretching and folding. This viewpoint allows particular insights into how efficient mixing may arise in non-turbulent flows (laminar Stokes or Darcy flows), and how the interactions of such fluid motions (technically termed stirring) with molecular diffusion can result in exponentially accelerated dispersion (or mixing) toward the homogeneous state. Enhanced mixing accelerates the rate at which chemical reagents come together and react, and so understanding the mechanisms by which chaotic advection can occur in hydrothermal systems is an important step in understanding the entire system. As dispersion is described by the advection–diffusion equation, the relevant dimensionless group is the Péclet number Pe which characterises the relative timescales of advection and diffusion. Typically, significant acceleration of mixing is observed above $Pe \sim 100$, which corresponds to a minimum pore or fracture length-scale L_{min} of order 1 mm in hydrothermal systems.

There are three distinct mechanisms by which fluid mixing can occur in hydrothermal systems: (i) via molecular diffusion of chemical species, (ii) via flow instabilities which arise from differences in physical properties at the concentration interface of chemical species, and (iii) via the fluid mechanics arising from flow through open porous and fractured networks. For pore length-scales $L > L_{min}$, dispersion via fluid mixing is typically several orders of magnitude larger than molecular diffusion alone (and this ratio scales as $\sqrt{Pe}$), and so mixing via molecular diffusion alone may be neglected in this regime. In the absence of fluid flow, the ADR system reduces to a reaction–diffusion system, and the literature regarding such systems is vast. Although reaction–diffusion dynamics are important in hydrothermal systems at very small scales, fluid advection has a significant role to play everywhere outside this regime.

The second mechanism is related to the formation of fluid interfaces in hydrothermal systems, where the intrusion or displacement of one fluid by another can form strong gradients in composition at these boundaries, and it is at these boundaries that chemical reaction typically occurs. These gradients and the associated reactions result in significant variations in temperature and in the concentration of chemical species, which in turn affect fluid physical properties including viscosity, density, and surface tension. Such gradients across the fluid interface admit a wide range of flow instabilities, and these instabilities promote fluid mixing which in turn further accelerates chemical reaction. As such, flow instabilities driven by chemical reaction form a positive feedback loop which promotes further mixing and reaction, and so efficient "mixing machines" form at fluid interfaces which propagate with the reaction front. Whilst the details and physico-chemical origin of these instabilities can vary widely, the unifying feature of these instabilities is that they can promote acceleration of mixing and reaction by several orders of magnitude. Such flow instabilities generate mixing or chaotic advection which is localised in time and space in that the instability is maintained so long as the causal gradients persist and is generally localised to the reaction front.

The third fluid mixing mechanism arises solely from the basic fluid mechanics of hydrothermal systems; this mechanism operates over a broad range of length scales, from the pore-scale to hundreds of kilometres. At the pore scale, steady flow within the complex geometry of open porous and fractured networks can generate chaotic advection through the basic elements of pore branching and recombination. Stokes flow through many of these topological features results in iterated stretching and folding of the fluid; these motions are the fundamental building blocks of chaotic advection. As such, steady flow in porous networks naturally creates material distributions with arbitrarily fine striations which, in conjunction with molecular diffusion, leads to exponentially accelerated mixing or dispersion. This dispersion in porous media is commonly termed hydrodynamic dispersion; however the underlying role of chaotic advection is not widely recognized as such. Therefore, fluid mixing is inherent to steady flow in hydrothermal systems at length-scales relevant to open porous and fractured networks, ranging from millimetres to tens of metres, but depends on the Péclet number as illustrated in Fig. 1.1.

It is important to note that both the 3D geometry of the network and Stokes flow within that network are necessary ingredients for steady flow to admit chaotic advection. Both of these assumptions are valid for these systems, but often practitioners use averaging over multiple length scales to develop formulations which involve either 2D geometry or Darcy flow. Whilst these approaches may be valid macroscopic approximations, use of these approximations prohibits (often unwittingly) chaotic advection in steady flows. However, transient Darcy flow in 2D or 3D does admit chaotic advection through flow reorientation which can again lead to stretching and folding and ultimately efficient mixing. Such flows are common at larger scales in hydrothermal systems, where punctuated or episodic fluid infiltration (Miller and Nur, 2000) leads to flow reorientation and efficient mixing.

As such, chaotic advection is inherent to hydrothermal mineralising systems and can arise via a range of mechanisms ranging from coupled physico-chemical flow instabilities through to steady Stokes flow within open porous and fractured networks, and large-scale transient Darcy flow at the regional scale. The direct impact of chaotic advection upon chemical reactions is to accelerate the rate of reaction through enhanced mixing, but also the filamentous nature of concentration distributions under chaotic advection acts fundamentally to alter the coupling between transport and reaction. As hydrothermal systems are open flow systems, the continual influx of fluid and chemical reagents means that non-equilibrium chemical conditions can be maintained indefinitely. In combination with these non-equilibrium chemical conditions, continuous flow though the reaction zone allows complex spatio-temporal distributions of chemical species to persist. The basic geometry of these structures has a significant impact upon the resultant coupled system. In the language of non-equilibrium thermodynamics, these distributions are dissipative structures which are maintained through the continual flux of energy and mass in the open hydrothermal system.

Chaotic advection in open flows involves net fluid flow through mixing regions, such that fluid particles undergo chaotic trajectories in this region but also their average motion is that of the net flow. The mixing region is characterised by the so-called *chaotic saddle*, a fractal set of closed orbits corresponding to the periodic points of the system, and so these orbits never leave the chaotic saddle. Associated with this set is the *unstable manifold* of the flow, another fractal object of zero volume which contains points which move asymptotically close to the saddle with decreasing time, $t \to -\infty$, and so fluid particles close to the unstable manifold are repelled from the chaotic saddle. In practical terms, the observed trajectories of dye molecules placed within the chaotic saddle would evolve to shadow the unstable manifold itself, and so the unstable manifold is responsible for organizing complex concentration distributions in open flows which admit chaotic advection. Although the unstable manifold has zero volume, concentration distributions on this manifold represent a "fattened up" manifold of finite volume, and it is at the interface of these filaments where chemical reaction occurs. This fractal geometry of concentration distributions leads to significantly altered reaction kinetics.

In the case of the autocatalytic reaction $A + B \to 2B$ with chemical species B injected into an open flow of constant concentration of A, the distribution of B very quickly conforms to shadow the unstable manifold of the flow. The autocatalytic reaction proceeds at the boundary of this distribution, and so long as species A and B are continually fed into the system the distribution of species B converges to a stationary spatio-temporal pattern which persists for all time. As the unstable manifold is fractal, the boundary of the B-species distribution on the

"fattened-up" manifold is very large, providing significant interfacial area for reactions to proceed. If the number N_B of B molecules decreases, the width of these "fattened-up" filaments also decreases toward the unstable manifold itself, and so the interfacial area and hence production of B grows without bound (as the unstable manifold is a fractal). As such, the rate of production of B grows as $N_B^{-\beta}$, where β is a positive number dependant only upon the fractal dimension D_f of the unstable manifold. Hence autocatalytic reactions in open flows which admit chaotic advection experience *singularly enhanced production* in that as species become rare, their rate of reaction increases toward infinity. This has significant implications for the stability of autocatalytic reactions in hydrothermal systems: so long as reactants are continually fed to maintain the system away from equilibrium, autocatalytic reactions are unconditionally stable to large perturbations and can persist for long times.

It is important to note that the phenomenon of singularly enhanced production arises solely from the fractal geometry of the unstable manifold, and not from the details of the chemical kinetics. In this light, it has been demonstrated that these principles apply to a wide range of non-equilibrium reactions relevant to hydrothermal systems, including competitive autocatalytic reactions, reactions with multiple stable equilibria and complex reactions involving catalysis (and inhibition) including thermal catalysis. The implication for hydrothermal systems is that singularly enhanced production due to chaotic advection in open flows acts to promote the stability and coexistence of reaction species by accelerating the production of species as their number reduces. For competitive autocatalytic and multi-stable reactions this means that all reaction species exist whilst non-equilibrium conditions are maintained.

As the unstable manifold does not move downstream with the flow itself, reactions are predominantly localised to the unstable manifold close to the region of the chaotic saddle. As such, mineral precipitation is localised to this region even in the advent of large flow rates. As precipitation reactions occur near the unstable manifold of the open flow, the spatial distribution of mineral deposits inherits the fractal geometry of the unstable manifold. For simple (i.e. smooth, regular) flows the unstable manifold has a single unique fractal dimension D_f which completely characterises the geometry of this object. Natural systems produce fractal distributions which typically do not possess a single fractal dimension but rather a spectrum of dimensions which change with the length-scale of interest. This makes intuitive sense as truly self-similar fractals (which have a unique fractal dimension) must be self-similar down to vanishingly small length-scales, that is, to the subatomic level and beyond. As such, the notion that the fractal dimension of objects can vary with length-scale is not particularly surprising, and such objects are described as being *multifractal*.

Flow in open porous and fractured networks is typically not smooth and regular due to the distribution of pore sizes and fractures. Typically these features are multifractally distributed in space, and so the attendant flows (either Stokesian or Darcy flow) in such systems are complex and generate unstable manifolds which are also multifractal. As such, mineral deposits are expected to be spatially distributed as multifractals due to the structure inherited by the unstable manifold, and indeed multifractal mineral deposits are observed in the field (Arias et al., 2011; Bastrakov et al., 2007; Ford and Blenkinsop, 2009; Hunt et al., 2007; Li et al., 2009; Oreskes and Einaudi, 1990; Qingfei et al., 2008; Riedi, 1998; Sanderson et al., 2008). An open question in this regard is how does the structure of the unstable manifold depend upon both the driving flow and the multifractal distribution of pore sizes in open porous and fractured networks.

Hence it is important to examine ore grade distributions from a multifractal viewpoint, but one must bear the physical and chemical processes in mind. Arneodo et al. (1995) point out that the geometrical process of establishing a multifractal distribution tends to filter or average the details of the physics behind the processes involved. The natural method here is the use of wavelet analysis with a thermodynamic foundation (Arneodo et al., 1995). Such methods have been applied to the analysis of banded structures in mineralised systems (Rusinov et al., 2006) but not so far to the analysis of ore grade. It is important to note that Arneodo et al. (1995) show that it is possible to extract from the data some information on the nature of the dynamical system responsible for the data, in particular the origin of the multiplicative hierarchical structure of some multifractals. Such studies hold the potential for increasing the understanding behind ore-grade distributions and in particular discovering if there is intrinsic structural order underlying what appears to be an irregular distribution of ore-grades rather than simply restrict one's considerations as to whether the ore distribution is spatially isotropic or anisotropic.

The assumption of ergodicity is invoked in many geostatistical applications despite warnings (e.g. Sposito, 1997; Truesdell, 1961) that ergodicity is a characteristic of the dynamical behaviour of a particular system rather than an assumption that can be used to rationalise the application of a probabilistic model. As such, it is of critical importance to establish whether or not hydrothermal mineralising systems give rise to mineral distributions which are ergodic. It is important to note that the precise meaning of the term ergodic is different when used in the context of measure-preserving transformations or stochastic processes. In the former case a process is ergodic if a spatial average of the process corresponds to the temporal average; as per the example of the Lyapunov exponent being constant in chaotic regions of the flow in Section 3.1. In terms of stochastic processes, a process is ergodic if multiple samples of the process on a finite region are representative of the process over the entire region. As such, ergodicity in the context of geostatistics refers to the ability to scale an ensemble of observed distributions to scales larger than the sample size. Consequently, the property of mineral deposits being multifractal also renders them non-ergodic in the context of geostatistics, as the fractal dimension of these deposits changes with the length-scale of interest. A similar problem is encountered in the scale-up of permeability distributions in porous media; if the permeability distribution is not truly self-similar, then the statistical basis for scaling the distribution up to larger scales is not sound, and only samples at larger scales can inform as to the distribution at that scale.

We have not devoted much space in this review to the complete solution of Eq. (2.1) where the diffusion process is coupled to the rates of production of chemical components by both reaction and advection. This is largely for lack of space since the topic is very large (Cross and Hohenberg, 1993; Epstein and Pojman, 1998; Fisher and Lasaga, 1981; Gray and Scott, 1990; Scott, 1994; Turing, 1952). Coupling with diffusion is capable of producing spatial patterning as is coupling with any process that advects or diffuses chemical components through the system. Deformation coupled to reaction plays the same role in developing spatial patterning (Ortoleva, 1994). At least at the millimetre and sub-millimetre scales some spatial patterning of alteration and of mineralisation may arise from such coupling. The patterns can be stripes (layers), lineations or blobs (Bansagi et al., 2011). Such patterns at the kilometre scale are likely to result from reaction–advection coupling. In particular Rusinov and Zhukov (2000, 2008) have modelled the development of banded wollastonite–hedenbergite skarns at the decimetre scale using a coupled reaction–advection model.

As indicated in Part I, in contrast to isolated and diffusive systems where the chemical reactions ultimately evolve to equilibrium under the imposed constraints, the chemical reactions in open flow systems evolve to one or more non-equilibrium stationary states. State selection is defined by the net flow rate (the product of the volumetric flow rate and species concentration) and by the nature of the chaotic flow system during fluid mixing. Various processes result in nonlinear chemical kinetics in any chemical system but the influence of the net flow in defining the stationary state in open flow systems results in highly nonlinear chemical systems that have many modes of stationary state behaviour depending on local conditions. The net flow rate

depends on the permeability and so slight local fluctuations in permeability can result in entirely different modes of chemical behaviour including little or no reaction, steady reaction at high yield (reaction extent), and oscillatory and chaotic behaviour at both high and low yield. Such strong dependence on local conditions also is apparent in spatial patterning. Oscillatory and chaotic behaviour are particularly important for mineralisation processes in well mixed systems. An example is where the mean environment is oxidised and acid with strong excursions into a reduced and alkaline environment. This leads to oscillatory or chaotic precipitation of sulphides and metals such as gold. The nonlinear dynamics of the system can produce spatial patterning where mean environments that are acid and oxidised are embedded in regions that are alkaline and reduced thus producing the strong gradients in Eh and pH observed in mineralising systems. This patterning is scale invariant and results from different phenomena operating at different scales but each producing the same range of nonlinear chemical behaviour at the relevant scale. Such processes include competitive reaction sites at crystal surfaces at the nanoscale, autocatalysis and thermal catalysis at intermediate scales and chaotic mixing at all scales above about 1 mm including the km-scale.

8. Concluding remarks

Evidently there are three goals in studying the fabric of a hydrothermal mineralising system. (i) One goal is to use the information within a particular system to discover similar mineralising systems elsewhere on Earth. (ii) A second objective is to use limited data within an individual system to "home in" on highly mineralised parts of that system. (iii) A third objective is to use limited data on the mineralised part of the system to estimate the total mineralised endowment of the system and its spatial distribution. The material covered by Parts I and II of this review show that hydrothermal mineralising systems are complex systems where a number of nonlinear reaction kinetics processes interact to produce what appear to be quite irregular spatial distributions of alteration and mineralisation at all spatial scales. We would like to know the answers to a number of questions regarding such systems: how best do we quantify the distributions of alteration, structures and mineralisation? In doing so can we gain deeper insight into the nature of the complexity of the system? Can we gain some insight into the underlying dynamical systems that resulted in the fabrics we see? Is it possible to characterise the nonlinear processes that developed the dynamical template that created the fabric we see? Is there any kind of universality in the fabric that enables us to use results at one scale to say useful things about other spatial scales? Is there an underlying unifying framework we can use to meet the three goals mentioned above?

We suggest that all of these questions can be answered in the near future but not within a framework based on equilibrium chemical thermodynamics. Hydrothermal mineralising systems are open flow systems that are driven according to well defined rules (involving a Lyapunov function [the Ross excess work] similar to the change in Gibbs energy, ΔG, relevant to systems approaching equilibrium) to non-equilibrium stationary states that may or may not be stable. The system never reaches equilibrium and only stops operating because the driving forces (external supplies of heat and mass) cease. The now well established theories of non-equilibrium systems need to be developed specifically for hydrothermal systems and applied to specific examples. The suggestion from this review is that mineralising systems form a spectrum between flow controlled and hydraulic potential controlled open flow systems and that they evolve through a number of modes of operation depending on the nature of the flow constraints. In general these modes of operation involve an early pervasive alteration of existing rocks such as the formation of sericite from feldspar or siderite from mafic rocks. This stage is essentially exothermic, is self-enhancing and can accommodate the imposed flow through the negative ΔV of chemical reactions and the maintenance of constant or elevating temperatures. Once this mode of operation ceases (due to exhaustion of initial minerals such as feldspar as reactants for the alteration) new modes of operation must operate to accommodate the imposed flow of heat and (particularly) mass. This commonly involves fracturing in some manner to produce veins, breccias or stockworks but is soon overprinted by numerous cycles of competitive endothermic and exothermic processes. The endothermic processes involve precipitation of sulphides (and/or metals) and anhydrous silicates that tend to kill the system. The exothermic processes involve formation of new carbonates and hydrous silicates (such as chlorite or biotite from sericite) and iron oxides; such competitive processes enhance the operation of the system and enable the continuous supply of fluids to be accommodated. The entire process is commonly autocatalytic in H^+ or is unstable due to other processes such as oxidation of Fe^{2+}, heterogeneous reactions at grain boundaries or thermal-catalysis arising from exothermic reactions so that a number of nonlinear chemical processes such as bistability, oscillatory or chaotic behaviour can arise controlled both by fluctuations in the permeability and the mode of mixing of nutrients. This unstable chemical behaviour results in Eh and pH gradients at all spatial scales from the nano-scale where it is important for metallurgical considerations to the mine- and regional-scales where it is important for exploration considerations. Understanding these modes of behaviour is fundamental to understanding whether a given system has been successful or has failed as an interesting mineral exploration target based on limited data.

Fluid mixing is undoubtedly an important aspect of the mineralising process but efficient fluid mixing is only possible with the proper three dimensional open plumbing networks; this can occur at the pore and micro-fracture scale up to the regional scale. The important point is that efficient mixing involves chaotic mixing and cannot occur simply by bringing two different fluids together in a steady Darcy flow. The chaotic mixing process at all spatial scales is important for controlling the precise form of mineral reactions (stable, bistable, oscillatory or chaotic). It is important to understand that the nutrients required for mineralisation can be premixed before entry to the mineralising system or can be fed independently and mixed in the system. The strong non-linearity characterising many of the reactions is such that premixed fluids can remain together for some time before reaction rates become significant. The reaction kinetics of many chemical systems in flow controlled units, namely, those that involve thermal- and/or auto-catalysis or competition between different reaction sites on a mineral surface, are such that subtle changes in net flow rate (the product of volumetric flow rate and chemical species concentration) can result in very large changes in reaction rate and the mode of reaction (stable, oscillatory, chaotic) so that the system may remain at low reaction rates before rapid reaction ensues. This means that for some critical net flow rates chaotic mixing can occur for extended periods before reaction begins. The chaotic mixing itself also influences the mode of chemical reaction so that the process acts as a state selection process between steady, bistable, oscillatory or chaotic modes along with the other important control (Part I) namely variations in local flow rate controlled by variations in permeability. The distinction between premixing and direct injection followed by mixing may be important from an exploration concept point of view since the mixing plumbing systems are quite different.

An extra layer of complexity is added by chaotic mixing arising from one or both of the mechanisms: (i) coupling of chemical reactions with physical properties such as viscosity, density and surface tension and (ii) non-smooth fluid flow in three dimensional systems of pores or fractures, through the process of flow branching and recombination, and in two and three dimensional Darcy flow where the fluid flow is episodic (punctuated). Chaotic flow means that fluid particles undergo chaotic trajectories although their average motion is that of the net flow. The flow is not turbulent. The result is the formation of a fractal set of orbits for the fluid particles and

the formation of arbitrarily fine striations of two or more fluids which in conjunction with molecular diffusion leads to accelerated mixing. The chemical reactions play out on this template. However there is a length scale, governed by the Péclet number, above which chemical reactions are enhanced by the mixing. Below this length scale, although chaotic mixing still occurs, chemical reactions are not enhanced by chaotic mixing and the chemical system is controlled solely by reaction–diffusion processes. In the chaotic mixing regime the fractal nature of the mixing provides an enhanced surface area for reactions to proceed. The competition between chemical reaction rates and exponential stretching of mixing striations leads to spatially stationary patterns that are not swept downstream with the flow. On this template, singularly enhanced production can proceed. Singularly enhanced production of chemical products occurs if the number of reactant molecules decreases because the surface area of the striations increases without bound. As indicated, the overall template does not move downstream with the flow but remains spatially invariant so that the enhanced mineralisation rate remains localised. The spatial invariance of the mixing template combined with singularly enhanced production and non-linear chemical system behaviour is responsible for locally high ore grades that appear to be irregularly distributed but which are multifractal. Such processes are enhanced at length scales typical of many hydrothermal systems and particularly for breccias. In simple flows the distribution of mineralisation is characterised by a single fractal dimension but in most open flows the distribution is multifractal due non-regular flow induced by irregularities in the pore or fracture geometry.

The ultimate objective of exploring a hydrothermal system is to solve the inverse problem of gaining insight into the nonlinear dynamical processes responsible for the mineralisation from limited observations made from drill hole or outcrop data. It seems that mineralising systems may be multifractal although considerable work is needed in this regard before any systematics will appear. Although such studies would be useful in order to obtain a statistical thermodynamic description of the mineralising process the geometrical process of performing fractal or multifractal analyses tends to smear or filter the information in the data and a more thermodynamic based process is needed to delve deeper into the complexity to extract details of the nonlinear dynamics of the system. A possible way forward involves the use of wavelets specifically constructed from the physical and chemical processes underlying the mineralising process. Present forms of kriging based on the assumption of ergodicity are unlikely to be useful in either delineating something of the underlying nonlinear dynamics or in accurately estimating ore reserves because the underlying dynamical systems are unlikely to be ergodic. Wavelet analysis based on the dynamics of the mineralising process offers a potentially important way forward.

Finally, hydrothermal ore systems should be considered as open flow chemical reactors held far from equilibrium by the supply of energy (heat) and mass (nutrients); Their evolution and final characteristics (successful or not, size, grade and grade distribution) can only be understood if the system is considered as one evolving in time. The successful systems are those that evolve through a series of stages involving competitive processes that enable the energy and efficiently mixed nutrients to be added to the system with evolving and increasing efficiency for as long as the system remains open. It is the recognition of these competitive chemical and structural modes of operation that enable one to recognise a failed from a successful system.

Acknowledgements

This project was funded under Australian Research Council (ARC) Linkage Project LP100200785, Multiscale Dynamics of Ore Body Formation, with support from The Geological Survey of Western Australia and Primary Industries and Resources South Australia (PIRSA). We would like to thank Ian Tyler, Catherine Spaggiari, Paul Heithersay and Tim Baker for continued support and discussions. Comments from Julian Vearncombe are much appreciated. The paper benefitted significantly from a careful review by Stephen Cox. We thank Tim Horscroft and Nigel Cook for the invitation to contribute this review.

Appendix

Table A1
Symbols used in the text with units.

Quantity	Description	Units
$\varkappa$	Number of chemical species	Dimensionless
a, b, c	Concentrations of chemical components A, B and C	Dimensionless or mol kg^{-3} or moles/unit volume of fluid
a_o, b_o, c_o	Initial concentrations of A, B and C	Dimensionless or mol kg^{-3} or moles/unit volume of fluid
c_i	Concentration of the i-th chemical species in solution	Dimensionless or mol kg^{-3} or moles/unit volume of fluid
$\boldsymbol{c}(\mathbf{r}, t)$	local concentration vector at the position defined by **r**	
c_1 c_2	Stationary states	
D	Mass or molecular diffusivity	$m^2\ s^{-1}$
D	Matrix of diffusive transport coefficients	$m^2\ s^{-1}$
D_i	diffusion coefficient	$m^2\ s^{-1}$
D_f	Fractal dimension	Dimensionless
D_u	Fractal dimension of the unstable manifold	Dimensionless
D_{eff}	Effective fractal dimension	Dimensionless
$\hat{\mathbf{e}}$	Unit vector along the unstable manifold direction	Dimensionless
Fi	quantifies the reaction kinetics of species i	
$\mathbf{f}(\boldsymbol{c}, b)$	vector function representing the reaction kinetics	
g, g	Acceleration due to gravity	$m^2\ s^{-1}$
$\mathcal{H}$	Hydraulic potential	Pa
H	Helicity	
K	Permeability	m^2
L	Characteristic length	m
M_b M_c	Mobility ratios	
$N(\varepsilon)$	Number of boxes required to cover the stable manifold	Dimensionless
p^{fluid}, $\hat{p}$	Fluid pressure	Pa
$\hat{\mathbf{s}}$	Unit vector along the stable manifold direction	Dimensionless
t	Time	s
$\hat{\mathbf{V}}$	Darcy flux	$m^3\ m^{-2}\ s^{-1}$
v; **v**	Fluid velocity; fluid velocity field	$m\ s^{-1}$
ν	Velocity of the propagating reaction front	$m\ s^{-1}$
$\boldsymbol{x}$, x	Coordinates	m
α β	constants	
α_k	weighting of each eigenmode	
κ	Escape rate	s^{-1}
μ	Fluid viscosity	Pa s
τ	Residence time	s
ρ	Density	$kg\ m^{-3}$
γ	Surface tension	$N\ m^{-1}$
$\boldsymbol{\omega}$	Vorticity	Dimensionless
ω_k	Characteristic rate of decay	s^{-1}
ϕ	Instantaneous porosity	Dimensionless
Ω	Pore space	
φ φ_n	Concentration field; concentration distribution	Dimensionless
$\varphi_k(\boldsymbol{x},t)$	Strange eigenmodes	
λ	Lyapunov exponent	Dimensionless
Λ	Local finite-time Lyapunov exponent measuring the stretching history	Dimensionless
ζ	Denotes Lagrangian coordinates	
∇	Gradient operator	
$\langle\rangle$	Denotes the averaging process	

References

Adler, R.J., 1981. The Geometry of Random Fields. Wiley, New York.

Adrover, A., Cerbelli, S., Giona, M., 2002a. A spectral approach to reaction/diffusion kinetics in chaotic flows. Comput. Chem. Eng. 26, 125–139.

Adrover, A., Continillo, G., Crescitelli, S., Giona, M., Russo, L., 2002b. Construction of approximate inertial manifold by decimation of collocation equations of distributed parameter systems. Comput. Chem. Eng. 26, 113–123.

Almarcha, C., Trevelyan, P.M.J., Grosfils, P., De Wit, A., 2010. Chemically driven hydrodynamic instabilities. Phys. Rev. Lett. 104.

Appold, M.S., Garven, G., 2000. Reactive flow models of ore formation in the Southeast Missouri district. Econ. Geol. Bull. Soc. Econ. Geol. 95, 1605–1626.

Aref, H., 1984. Stirring by chaotic advection. J. Fluid Mech. 143, 1–21.

Arias, M., Gumiel, P., Sanderson, D.J., Martin-Izard, A., 2011. A multifractal simulation model for the distribution of VMS deposits in the Spanish segment of the Iberian Pyrite Belt. Comput. Geosci. 37, 1917–1927.

Arneodo, A., Bacry, E., Muzy, J.F., 1995. The thermodynamics of fractals revisited with wavelets. Physica A 213, 232–275.

Arratia, P.E., Gollub, J.P., 2006. Predicting the progress of diffusively limited chemical reactions in the presence of chaotic advection — art. no. 024501. Phys. Rev. Lett. 9602, 4501-.

Bansagi, T., Vanag, V.K., Epstein, I.R., 2011. Tomography of reaction–diffusion microemulsions reveals three-dimensional Turing patterns. Science 331, 1309–1312.

Barnicoat, A.C., Henderson, I.H.C., Knipe, R.J., Yardley, B.W.D., Napier, R.W., Fox, N.P.C., et al., 1997. Hydrothermal gold mineralization in the Witwatersrand basin. Nature 386, 820–824.

Bastrakov, E.N., Skirrow, R.G., Didson, G.J., 2007. Fluid evolution and origins of iron oxide Cu–Au prospects in the Olympic Dam district, Gawler craton, south Australia. Econ. Geol. 102, 1415–1440.

Bear, J., 1972. Dynamics of Fluids Porous Media. Elsevier, New York, USA.

Benard, H., 1900a. Experimental studies on the movement of liquids propagated by heat by means of convection. Permanent system : Cellular turbulence. C. R. Hebd. Seances Acad. Sci. 130, 1004–1007.

Benard, H., 1900b. Swirling movements of cellular structure. Optic study of free surfaces. C. R. Hebd. Seances Acad. Sci. 130, 1065–1068.

Berti, S., Vergni, D., Visconti, F., Vulpiani, A., 2005. Mixing and reaction efficiency in closed domains — art. no. 036302. Phys. Rev. E 7203, 6302-.

Bockmann, M., Muller, S.C., 2000. Growth rates of the buoyancy-driven instability of an autocatalytic reaction front in a narrow cell. Phys. Rev. Lett. 85, 2506–2509.

Borckmans, P., Dewel, G., De Wit, A., Dulos, E., Boissonade, J., Gauffre, F., et al., 2002. Diffusive instabilities and chemical reactions. Int. J. Bifurcation Chaos 12, 2307–2332.

Carlson, C.A., 1991. Spatial distribution of ore deposits. Geology 19, 111–114.

Carrière, P., 2007. On a three-dimensional implementation of the baker's transformation. Phys. Fluids 19, 118110.

Cerbelli, S., Giona, M., 2009. On the connection between reaction efficiency and interface structure in open laminar flows. Comput. Chem. Eng. 33, 333–346.

Cerbelli, S., Vitacolonna, V., Adrover, A., Giona, M., 2004. Eigenvalue–eigenfunction analysis of infinitely fast reactions and micromixing regimes in regular and chaotic bounded flows. Chem. Eng. Sci. 59, 2125–2144.

Cerbelli, S., Garofalo, F., Giona, M., 2008. Steady-state performance of an infinitely fast reaction in a three-dimensional open Stokes flow. Chem. Eng. Sci. 63, 4396–4411.

Clifford, M.J., Cox, S.M., Roberts, E.P.L., 1998. Lamellar modelling of reaction, diffusion and mixing in a two-dimensional flow. Chem. Eng. J. 71, 49–56.

Clifford, M.J., Cox, S.M., Roberts, E.P.L., 2000. The influence of a lamellar structure upon the yield of a chemical reaction. Chem. Eng. Res. Des. 78, 371–377.

Cox, S.F., 1995. Faulting processes at high fluid pressures — an example of fault valve behavior from the Wattle Gully fault, Victoria, Australia. J. Geophys. Res. Solid Earth 100, 12841–12859.

Cox, S.M., 2004. Chaotic mixing of a competitive–consecutive reaction. Physica D 199, 369–386.

Cox, S.M., Gottwald, G.A., 2006. A bistable reaction–diffusion system in a stretching flow. Physica D 216, 307–318.

Cox, S., Ruming, K., 2004. The St Ives mesothermal gold system, Western Australia — a case of golden aftershocks? J. Struct. Geol. 26, 1109–1125.

Cressie, N.A.C., 1993. Statistics for Spatial Data, Revised ed. John Wiley & Sons, Inc., New York.

Cressie, N., Wikle, C., 2011. Statistics for Spatio-Temporal Data. Wiley, Hoboken, NJ.

Cross, M., Greenside, H., 2009. Pattern Formation and Dynamics in Nonequilibrium Systems. Cambridge University Press, Cambridge, UK.

Cross, M.C., Hohenberg, P.C., 1993. Pattern formation outside of equilibrium. Rev. Mod. Phys. 65, 851–1112.

de Moura, A.P.S., Grebogi, C., 2004a. Chemical and biological activity in three-dimensional flows — art. no. 026218. Phys. Rev. E 7002, 6218-.

de Moura, A.P.S., Grebogi, C., 2004b. Reactions in flows with nonhyperbolic dynamics — art. no. 036216. Phys. Rev. E 7003, 6216-.

De Wit, A., 2001. Fingering of chemical fronts in porous media. Phys. Rev. Lett. 87.

De Wit, A., 2004. Miscible density fingering of chemical fronts in porous media: nonlinear simulations. Phys. Fluids 16, 163–175.

De Wit, A., 2008. Chemi-hydrodynamic patterns and instabilities. Chim. Nouv. 9, 1–7.

De Wit, A., Homsy, G.M., 1999a. Nonlinear interactions of chemical reactions and viscous fingering in porous media. Phys. Fluids 11, 949–951.

De Wit, A., Homsy, G.M., 1999b. Viscous fingering in reaction–diffusion systems. J. Chem. Phys. 110, 8663–8675.

De Wit, A., De Kepper, P., Benyaich, K., Dewel, G., Borckmans, P., 2003. Hydrodynamical instability of spatially extended bistable chemical systems. Chem. Eng. Sci. 58, 4823–4831.

Demuth, R., Meiburg, E., 2003. Chemical fronts in Hele–Shaw cells: linear stability analysis based on the three-dimensional Stokes equations. Phys. Fluids 15, 597–602.

D'Hernoncourt, J., Zebib, A., De Wit, A., 2007. On the classification of buoyancy-driven chemo-hydrodynamic instabilities of chemical fronts. Chaos 17.

Dube, B., Goselin, P., 2007. Greenstone-hosted quartz–carbonate vein deposits. In: Goodfellow, W.D. (Ed.), Mineral Deposits of Canada: A Synthesis of Major Deposit-Types, District Metallogeny, the Evolution of Geological Provinces, and Exploration Methods. Geological Association of Canada, Mineral Deposits Division, pp. 49–73.

Eastoe, C.J., Solomon, M., Walshe, J.L., 1987. District-scale alteration associated with massive sulfide deposits in the Mount Read Volcanics. Western Tasmania Econ. Geol. 82, 1239–1258.

Epstein, I.R., Pojman, J.A., 1998. An Introduction to Nonlinear Chemical Dynamics: Oscillations, Waves, Patterns, and Chaos. Oxford University Press, Oxford.

Fields, S.D., Ottino, J.M., 1987a. Effect of stretching path on the course of polymerizations: applications to idealized unpremixed reactors. Chem. Eng. Sci. 42, 467–477.

Fields, S.D., Ottino, J.M., 1987b. Effect of striation thickness distribution on the course of an unpremixed polymerization. Chem. Eng. Sci. 42, 459–465.

Fields, S.D., Ottino, J.M., 1987c. Mixing effects during polymerization by the adiabatic temperature rise technique. AIChE J. 33, 157–160.

Finn, M.D., Cox, S.M., 2011. Shear-flow suppression of hotspot growth. Physica D 240, 709–718.

Fisher, G.W., Lasaga, A.C., 1981. Irreversible thermodynamics in petrology. Rev. Mineral. Geochem. 8, 171–207.

Ford, A., Blenkinsop, T.G., 2009. An expanded de Wijs model for multifractal analysis of mineral production data. Miner. Deposita 44, 233–240.

Galaktionov, O.S., Anderson, P.D., Peters, G.W.M., Van de Vosse, F.N., 2000. An adaptive front tracking technique for three-dimensional transient flows. Int. J. Num. Methods Fluids 32, 201–217.

Garrison, S., 2001. Topological groundwater hydrodynamics. Adv. Water Res. 24, 793–801.

Gray, P., Scott, S.K., 1990. Chemical Oscillations and Instabilities. Oxford University Press, Oxford.

Haynes, D.W., Cross, K.C., Bills, R.T., Reed, M.H., 1995. Olympic Dam ore genesis — a fluid-mixing model. Econ. Geol. Bull. Soc. Econ. Geol. 90, 281–307.

Henley, R.W., Berger, B.R., 2000. Self-ordering and complexity in epizonal mineral deposits. Annu. Rev. Earth Planet. Sci. 28, 669–719.

Hernandez-Garcia, E., Lopez, C., 2004. Sustained plankton blooms under open chaotic flows. Ecol. Complexity 1, 253–259.

Hillary, R.M., Bees, M.A., 2004. Plankton lattices and the role of chaos in plankton patchiness — art. no. 031913. Phys. Rev. E 6903, 1913-.

Hunt, J.A., Baker, T., Thorkelson, D.J., 2007. A review of iron oxide copper–gold deposits, with focus on the Wernecke Breccias, Yukon, Canada, as an example of a non-magmatic end member and implications for IOCG genesis and classification. Explor. Min. Geol. 16, 209–232.

Iordanidis, A.A., Annaland, M.V., Kronberg, A.E., Kuipers, J.A.M., 2004. A numerical method for the solution of the wave model and convection dominated diffusion type models for catalytic packed bed reactors. Comput. Chem. Eng. 28, 2337–2349.

Jones, S., Aref, H., 1988. Chaotic advection in pulsed source-sink systems. Phys. Fluids 31, 469–485.

Karolyi, G., Tel, T., 2007. Effective dimensions and chemical reactions in fluid flows — art. no. 046315. Phys. Rev. E 76, 6315-.

Karolyi, G., Pentek, A., Toroczkai, Z., Tel, T., Grebogi, C., 1999. Chemical or biological activity in open chaotic flows. Phys. Rev. E 59, 5468–5481.

Karolyi, G., Tel, T., de Moura, A.P.S., Grebogi, C., 2004. Reactive particles in random flows — art. no. 174101. Phys. Rev. Lett. 9217, 4101-.

Karolyi, G., Neufeld, Z., Scheuring, I., 2005. Rock–scissors–paper game in a chaotic flow: the effect of dispersion on the cyclic competition of microorganisms. J. Theor. Biol. 236, 12–20.

Kiss, I.Z., Merkin, J.H., Neufeld, Z., 2003a. Combustion initiation and extinction in a 2D chaotic flow. Physica D 183, 175–189.

Kiss, I.Z., Merkin, J.H., Scott, S.K., Simon, P.L., Kalliadasis, S., Neufeld, Z., 2003b. The structure of flame filaments in chaotic flows. Physica D 176, 67–81.

Kiss, I.Z., Merkin, J.H., Neufeld, Z., 2004. Homogenization induced by chaotic mixing and diffusion in an oscillatory chemical reaction — art. no. 026216. Phys. Rev. E 7002, 6216-.

Large, R.R., Gemmell, J.B., Paulick, H., Huston, D.L., 2001. The alteration box plot: a simple approach to understanding the relationship between alteration mineralogy and lithogeochemistry associated with volcanic-hosted massive sulfide deposits. Econ. Geol. Bull. Soc. Econ. Geol. 96, 957–971.

Lester, D.R., Rudman, M., Metcalfe, G., Blackburn, H.M., 2008. Global parametric solutions of scalar transport. J. Comput. Phys. 227, 3032–3057.

Lester, D.R., Metcalfe, G., Trefry, M.G., Ord, A., Hobbs, B., Rudman, M., 2009. Lagrangian topology of a periodically reoriented potential flow: symmetry, optimization, and mixing. Phys. Rev. E 80, 036208.

Lester, D.R., Rudman, M., Metcalfe, G., Trefry, M.G., Ord, A., Hobbs, B., 2010. Scalar dispersion in a periodically reoriented potential flow: acceleration via Lagrangian chaos. Phys. Rev. E 81, 046319.

Li, W., Jun, D., Qingfei, W., 2009. Multifractal modeling and evaluation of inhomogeneity of metallogenic elements distribution in the Shangzhuang Deposit, Shandong Province, China. Computational Intelligence and Software Engineering, 2009 CiSE 2009 International Conference, pp. 1–4.

Liu, W., Haller, G., 2004. Strange eigenmodes and decay of variance in the mixing of diffusive tracers. Physica D 188, 1–39.

Lopez, C., Hernandez-Garcia, E., 2002. The role of diffusion in the chaotic advection of a passive scalar with finite lifetime. Eur. Phys. J. B 28, 353–359.

Lopez, C., Hernandez-Garcia, E., Piro, O., Vulpiani, A., Zambianchi, E., 2001. Population dynamics advected by chaotic flows: a discrete-time map approach. Chaos 11, 397–403.
MacKay, R.S., 2001. Complicated dynamics from simple topological hypotheses. Philos. Transact. A Math. Phys. Eng. Sci. 359, 1479–1496.
Manning, C.E., Ingebritsen, S.E., 1999. Permeability of the continental crust: Implications of geothermal data and metamorphic systems. Rev. Geophys. 37, 127–150.
Martin, A.P., 2003. Phytoplankton patchiness: the role of lateral stirring and mixing. Prog. Oceanogr. 57, 125–174.
Menon, S.N., Gottwald, G.A., 2005. Bifurcations in reaction–diffusion systems in chaotic flows — art. no. 066201. Phys. Rev. E 7106, 6201-.
Menon, S.N., Gottwald, G.A., 2009. On bifurcations in a chaotically stirred excitable medium. Physica D 238, 461–475.
Metcalfe, G., 2010. Applied fluid chaos: designing advection with periodically reoriented flows for micro to geophysical mixing and transport enhancement. In: Dewar, R.L., Detering, F. (Eds.), Complex Physical, Biophysical and Econophysical Systems Proceedings of the 22nd Canberra International Physics Summer School. World Scientific, Canberra, pp. 187–239.
Metcalfe, G., Lester, D., Ord, A., Kulkarni, P., Rudman, M., Trefry, M., et al., 2010a. An experimental and theoretical study of the mixing characteristics of a periodically reoriented irrotational flow. Philos. Trans. R. Soc. Lond. A 368, 2147–2162.
Metcalfe, G., Lester, D., Ord, A., Kulkarni, P., Trefry, M., Hobbs, B.E., et al., 2010b. A partially open porous media flow with chaotic advection: towards a model of coupled fields. Philos. Trans. R. Soc. Lond. A 368, 217–230.
Mezić, I., 1999. Residence-time distributions for chaotic flows in pipes. Chaos 9, 173.
Mezić, I., Loire, S., Fonoberov, V.A., Hogan, P., 2010. A new mixing diagnostic and Gulf Oil spill movement. Science 330, 486–489.
Miller, S.A., Nur, A., 2000. Permeability as a toggle switch in fluid-controlled crustal processes. Earth Planet. Sci. Lett. 183, 133–146.
Mishra, M., Trevelyan, P.M.J., Almarcha, C., De Wit, A., 2010. Influence of double diffusive effects on miscible viscous fingering. Phys. Rev. Lett. 105.
Moffatt, H.K., 1969. The degree of knottedness of tangled vortex lines. J. Fluid Mech. 35, 117–129.
Muntean, J.L., Cline, J.S., Simon, A.C., Longo, A.A., 2011. Magmatic-hydrothermal origin of Nevada's Carlin-type gold deposits. Nat. Geosci. 4, 122–127.
Muzzio, F.J., Liu, M., 1996. Chemical reactions in chaotic flows. Chem. Eng. J. Biochem. Eng. J. 64, 117–127.
Muzzio, F.J., Ottino, J.M., 1989. Evolution of a lamellar system with diffusion and reaction: a scaling approach. Phys. Rev. Lett. 63, 47–50.
Muzzio, F.J., Ottino, J.M., 1990. Diffusion and reaction in a lamellar system: self-similarity with finite rates of reaction. Phys. Rev. A 42, 5873–5884.
Muzzio, F.J., Meneveau, C., Swanson, P.D., Ottino, J.M., 1992. Scaling and multifractal properties of mixing in chaotic flows. Phys. Fluids Fluid Dyn. 4, 1439–1456.
Nagatsu, Y., De Wit, A., 2011. Viscous fingering of a miscible reactive A + B -> C interface for an infinitely fast chemical reaction: nonlinear simulations. Phys. Fluids 23.
Nagatsu, Y., Matsuda, K., Kato, Y., Tada, Y., 2007. Experimental study on miscible viscous fingering involving viscosity changes induced by variations in chemical species concentrations due to chemical reactions. J. Fluid Mech. 571, 475–493.
Nagatsu, Y., Kondo, Y., Kato, Y., Tada, Y., 2009. Effects of moderate Damkohler number on miscible viscous fingering involving viscosity decrease due to a chemical reaction. J. Fluid Mech. 625, 97–124.
Neufeld, Z., 2001. Excitable media in a chaotic flow. Phys. Rev. Lett. 87, 108301.
Neufeld, Z., Haynes, P.H., Tel, T., 2002. Chaotic mixing induced transitions in reaction–diffusion systems. Chaos 12, 426–438.
Neuman, S.P., Tartakovsky, D.M., 2009. Perspective on theories of non-Fickian transport in heterogeneous media. Adv. Water Resour. 32, 670–680.
Neumayr, P., Petersen, K.J., Gauthier, L., Hodge, J., Hagemann, S.G., Walshe, J.L., et al., 2005. Mapping of hydrothermal alteration and geochemical gradients as a tool for conceptual targeting: St Ives Gold Camp, Western Australia. Springer-Verlag Berlin, Berlin.
Neumayr, P., Walshe, J., Hagemann, S., Petersen, K., Roache, A., Frikken, P., et al., 2008. Oxidized and reduced mineral assemblages in greenstone belt rocks of the St. Ives gold camp, Western Australia: vectors to high-grade ore bodies in Archaean gold deposits? Miner. Deposita 43, 363–371.
Ord, A., Henley, S., 1997. Fluid pumping: some exploratory numerical models. Phys. Chem. Earth 22, 49–56.
Ord, A., Hobbs, B., Walshe, J., Metcalfe, G., Trefry, M., Zhao, C.B., et al., 2010. Architecture and mixing for crustal plumbing systems: St Ives as a type example. Smart Sci. Explor. Min. 833–835.
Oreskes, N., Einaudi, M.T., 1990. Origin of rare earth element-enriched hematite breccias at the Olympic Dam Cu–U–Au–Ag deposit, Roxby Downs, South Australia. Econ. Geol. 85, 1–28.
Ortoleva, P.J., 1994. Geochemical Self-Organisation. Oxford University Press, Oxford.
Ottino, J.M., 1989. The Kinematics of Mixing: Stretching, Chaos, and Transport. Cambridge University Press, Cambridge, UK.
Ottino, J.M., 1990. The Kinematics of Mixing: Stretching, Chaos, and Transport. Cambridge University Press, Cambridge, UK.
Ottino, J.M., 1994. Mixing and chemical reactions: a tutorial. Chem. Eng. Sci. 49, 4005–4027.
Pentek, A., Karolyi, G., Scheuring, I., Tel, T., Toroczkai, Z., Kadtke, J., et al., 1999. Fractality, chaos, and reactions in imperfectly mixed open hydrodynamical flows. Physica A 274, 120–131.
Pierrehumbert, R.T., 1994. Tracer microstructure in the large-eddy dominated regime. Chaos, Solitons Fractals 4, 1091–1110.
Pojman, J.A., 1990. A simple demonstration of convective effects on reaction–diffusion systems: a burning cigarette. J. Chem. Educ. 67, 792–794.
Pojman, J.A., Epstein, I.R., 1990. Convective effects on chemical waves. 1. Mechanisms and stability criteria. J. Phys. Chem. 94, 4966–4972.
Pompano, R.R., Li, H.-W., Ismagilov, R.F., 2008. Rate of mixing controls rate and outcome of autocatalytic processes: theory and microfluidic experiments with chemical reactions and blood coagulation. Biophys. J. 95, 1531–1543.
Prendergast, K., 2007. Application of lithogeochemistry to gold exploration in the St Ives Goldfield, Western Australia. Geochem. Explor. Environ. Anal. 7, 99–108.
Qingfei, W., Jun, D., Li, W.A.N., Jie, Z., Qingjie, G., Liqiang, Y., et al., 2008. Multifractal analysis of element distribution in skarn-type deposits in the Shizishan Orefield, Tongling Area, Anhui Province, China. Acta Geolog. Sin. English Ed. 82, 896–905.
Rayleigh, 1882. Investigation of the character of the equilibrium of an incompressible heavy fluid of variable density. Proc. Lond. Math. Soc. s1-14, 170–177.
Rayleigh, L., 1916. On convection currents in a horizontal layer of fluid, when the higher temperature is on the under side. Philos. Mag. 32, 529–546.
Reich, M., Kesler, S., Utsunomiya, S., Palenik, C., Chryssoulis, S., Ewing, R., 2005. Solubility of gold in arsenian pyrite. Geochim. Cosmochim. Acta 69, 2781–2796.
Riedi, R.H., 1998. Multifractals and wavelets: a potential tool in geophysics. SEG Conference. New Orleans, LA.
Rongy, L., De Wit, A., 2006. Steady Marangoni flow traveling with chemical fronts. J. Chem. Phys. 124.
Rongy, L., De Wit, A., 2007. Marangoni flow around chemical fronts traveling in thin solution layers: influence of the liquid depth. J. Eng. Math. 59, 221–227.
Rongy, L., De Wit, A., 2008. Solitary Marangoni-driven convective structures in bistable chemical systems. Phys. Rev. E 77.
Rongy, L., De Wit, A., 2009. Buoyancy-driven convection around exothermic autocatalytic chemical fronts traveling horizontally in covered thin solution layers. J. Chem. Phys. 131.
Rusinov, V.L., Zhukov, V.V., 2000. Dynamic model of the infiltration metasomatic zonation. Pure Appl. Geophys. 157, 637–652.
Rusinov, V.L., Zhukov, V.V., 2008. Model for the development of rhythmically banded wollastonite–hedenbergite skarns at the Dal'negorsk deposit, southern Russian Far East. Geochem. Int. 46, 789–799.
Rusinov, V.L., Bityutskaya, L.A., Bogatikov, E.V., Zhukov, V.V., 2006. Fractal features and morphological differences between periodic infiltration and diffusion metasomatic zonation. Dokl. Earth Sci. 409, 769–773.
Saffman, P.G., Taylor, G., 1958. The penetration of a fluid into a porous medium or Hele–Shaw cell containing a more viscous liquid. Proc. R. Soc. Lond., Ser. A Math. Phys. Sci. 245, 312-&.
Sanderson, D.J., Roberts, S., Gumiel, P., Greenfield, C., 2008. Quantitative analysis of tin- and tungsten-bearing sheeted vein systems. Econ. Geol. 103, 1043–1056.
Scheuring, I., Karolyi, G., Toroczkai, Z., Tel, T., Pentek, A., 2003. Competing populations in flows with chaotic mixing. Theor. Popul. Biol. 63, 77–90.
Schodde, R.C., Hronsky, J.M.A., 2006. The role of world-class mines in wealth creation. In: Doggett, M.D., Parry, J.R. (Eds.), Wealth Creation in the Minerals Industry: Integrating Science, Business, and Education. Soc Economic Geologists, Inc., Littleton, pp. 71–90.
Scott, S.K., 1994. Oscillations, Waves, and Chaos in Chemical Kinetics. Oxford University Press, Oxford.
Sibson, R.H., 1987. Earthquake rupturing as a mineralizing agent in hydrothermal systems. Geology 15, 701–704.
Sibson, R., 2007. An episode of fault-valve behaviour during compressional inversion? — The 2004 MJ6.8 Mid-Niigata Prefecture, Japan, earthquake sequence. Earth Planet. Sci. Lett. 257, 188–199.
Singh, M.K., Galaktionov, O.S., Meijer, H.E.H., Anderson, P.D., 2009. A simplified approach to compute distribution matrices for the mapping method. Comput. Chem. Eng. 33, 1354–1362.
Sokolov, I.M., Blumen, A., 1991a. Mixing effects in the A + B -> 0 reaction–diffusion scheme. Phys. Rev. Lett. 66, 1942–1945.
Sokolov, I.M., Blumen, A., 1991b. Reactions in systems with mixing. J. Phys. A Math. Gen. 24, 3687.
Sokolov, I.M., Blumen, A., 1991c. Structure of layered systems under reactions. Spontaneous Formation of Space–Time Structures and Criticality. Springer, Netherlands, pp. 203–206.
Sposito, G., 1994. Steady groundwater flow as a dynamical system. Water Resour. Res. 30, 2395–2401.
Sposito, G., 1997. Ergodicity and the 'scale effect'. Adv. Water Resour. 20, 309–316.
Tang, X.Z., Boozer, A.H., 1996. Finite time Lyapunov exponent and advection–diffusion equation. Physica D 95, 283–305.
Tang, X.Z., Boozer, A.H., 1999. A Lagrangian analysis of advection–diffusion equation for a three dimensional chaotic flow. Phys. Fluids 11, 1418–1434.
Taylor, G., 1950. The instability of liquid surfaces when accelerated in a direction perpendicular to their planes. I. Proc. R. Soc. Lond. A Math. Phys. Sci. 201, 192–196.
Tel, T., Karolyi, G., Pentek, A., Scheuring, I., Toroczkai, Z., Grebogi, C., et al., 2000. Chaotic advection, diffusion, and reactions in open flows. Chaos 10, 89–98.
Tel, T., de Moura, A., Grebogi, C., Karolyi, G., 2005. Chemical and biological activity in open flows: a dynamical system approach. Phys. Rep. Rev. Sect. Phys. Lett. 413, 91–196.
Thiffeault, J.-L., 2010. Chaos in the Gulf. Science 330, 458–459.
Toroczkai, Z., Karolyi, G., Pentek, A., Tel, T., 2001. Autocatalytic reactions in systems with hyperbolic mixing: exact results for the active Baker map. J. Phys. A Math. Gen. 34, 5215–5235.
Trefry, M.G., Lester, D.R., Metcalfe, G., Ord, A., Regenauer-Lieb, K., 2012. Toward enhanced subsurface intervention methods using chaotic advection. J. Contam. Hydrol. 127, 15–29.
Truesdell, C., 1961. Ergodic theory in classical statistical mechanics. In: Caldirola, P. (Ed.), Ergodic Theories. Academic Press, New York, pp. 21–56.

Tsang, Y.K., 2009. Predicting the evolution of fast chemical reactions in chaotic flows — art. no. 026305. Phys. Rev. E 80, 6305-.
Turing, A.M., 1952. The chemical basis of morphogenesis. Philos. Trans. R. Soc. Lond. B Biol. Sci. 237, 37–72.
Van den Bleek, C.M., Schouten, J.C., 1993. Deterministic chaos — a new tool in fluidized-bed design and operation. Chem. Eng. J. Biochem. Eng. J. 53, 75–87.
Villermaux, E., 2012. On dissipation in stirred mixtures. In: Erik van der, G., Hassan, A. (Eds.), Advances in Applied Mechanics. Elsevier, pp. 91–107.
Vollmer, J., 2002. Chaos, spatial extension, transport, and non-equilibrium thermodynamics. Phys. Rep. 372, 131–267.
Wiggins, S., Ottino, J.M., 2004. Foundations of chaotic mixing. Philos. Transact. A Math. Phys. Eng. Sci. 362, 937–970.
Zhang, P., DeVries, S.L., Dathe, A., Bagtzoglou, A.C., 2009. Enhanced mixing and plume containment in porous media under time-dependent oscillatory flow. Environ. Sci. Technol. 43, 6283–6288.